PRATHAM
IIT BOMBAY STUDENT SATELLITE

Report
Attitude Determination and Control System (ADCS)

By

Pratham Team

Department of Aerospace Engineering,

Indian Institute of Technology, Bombay

Sep 2015

Contents

List of Tables

List of Figures

Chapter 1

Pratham overview

In this chapter, we will give a brief introduction about the pratham satellite.

1.1 Vital Statistics about Pratham

Pratham is the first Student Satellite being built under the IIT Bombay Student Satellite Project. Some of the vital statistics about the Satellite are as follows:

- Weight 9.774 kg
- Size: 26 cm X 26 cm X 26 cm cube
- LVI from VSSC (IBL230V2)
- Solar Panels (4 sides)
- Orbit – 10:30 polar sun-synchoronous
- 3 pre-deployed monopoles (outside the 26 cm cube)
- Downlink at frequency 437.455 MHz
- Beacon at frequency 145.98 MHz
- Uplink at frequency 437.455 MHz
- Completely autonomous (except kill switch)

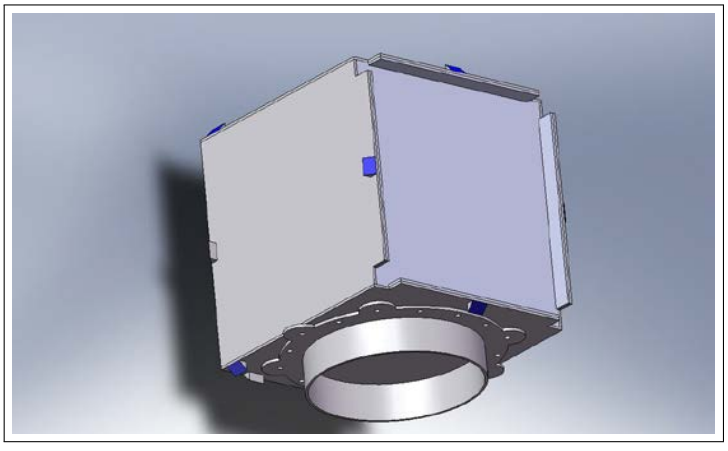

Figure 1.1: Pratham's Engineering Drawing

Chapter 2

Introduction to ADCS

2.1 Objectives:

- Position determination - To determine the position of the satellite in space, with respect to an inertial reference frame.
- Attitude Determination - To determine the attitude of the body frame of the satellite with respect to orbit frame.
- Attitude control - To bring the satellite into earth pointing orientation after ejection and to maintain this attitude within given bounds throughout the period of operation.

2.2 Requirements from other subsystems:

Requirements on the Attitude Determination and Controls Sub-System from the System

- Attitude Determination and Controls Sub-System shall stabilize the attitude within $\pm 10^o$ accuracy along all axes.
- They shall measure and control the instantaneous position of the Satellite in orbit to 1 kilometer accuracy.

Requirements from Communication and Ground Station Sub-System to Attitude Determination and Controls Sub-System

- Attitude Determination and Controls Sub-System shall maintain the Satellite at 0^0 pitch and 0^0 roll along the orbit reference frame, with a maximum error of ± 10 deg in both these axes.

Requirements from Payload Sub-System to Attitude Determination and Controls Sub-System

- Attitude Determination and Controls Sub-System shall maintain the Satellite at 0^0 yaw along the orbit reference frame, with a maximum error of ± 10 deg in this axes.

Requirements from Power Sub-System to Attitude Determination and Controls Sub-System

- During Mode 2, Attitude Determination and Controls Sub-System shall try to achieve an attitude such that maximum solar irradiation falls on the solar panels.

2.3 Requirements from ADCS subsystem to other subsystems:

Requirements from Attitude Determination and Controls Sub-System to On Board Computer Sub-System

- OBC Sub-System shall execute the Control Law as per the operational sequence.
- They shall interface with the following sensors:
  - Magnetometer (UART)
  - GPS (UART)
  - 6 Sun-Sensors (1 ADC with multiplexer)
- They shall drive the 3 magnetorquers using PWM.

Requirements from Attitude Determination and Controls Sub-System to Integration Sub-System

- Integration Team shall make the principal axis of the Satellite coincide with the geometric axis.
- They shall make the Satellite meet the conditions for Static stability, namely
  - $I_x > I_y > I_z$
  - $I_x < I_y + I_z$
- They shall place the 3 magnetorquers on 3 sides along the 3 body axis, namely the zenith, the leading velocity and the sun-side.
- They shall place the GPS on zenith and expose the antenna to space.
- They shall place the magnetometer at the position with least magnetic disturbances.
- They shall place the 6 Sun-Sensors on the 6 faces such that their field of view is not curtailed.

2.4 Requirement summary

- Position requirements are required by the communication subsystem to know when to begin data transmission when over a ground station.
- Requirements of the ADCS subsystem arise due to need for obtaining the components of earth's magnetic field and the sun vector in the orbit frame. This is required for attitude determination.

- Requirements of the payload subsystem arise due to the need for correlating the position of satellite with the measured value of TEC. This data is required on ground for post processing of the TEC data. Hence, either position must be calculated on ground using an orbit estimator or must be transmitted to ground from the satellite.

Requirement	**Imposed by**
Roll	Payload & communication subsystem
Pitch	Payload & communication subsystem
Yaw	Power subsystem
Position	Payload & communication subsystem

2.4.1 Attitude determination:

On board		
ADCS	Roll pitch Yaw	5 degrees (not stringent as long as control is obtained within desired limits)

- This is required to achieve attitude control of the satellite.

2.4.2 Attitude control:

Payload	10 deg (Roll, Pitch, Yaw)
Communication	10 deg (Roll, Pitch)

- Yaw stabilization is required by the payload.
- Roll and pitch stabilization is required by the communication subsystem to ensure proper signal reception from the satellite.

2.5 Reference frames and axis conventions

2.5.1 Satellite model

2.5.2 Reference Frames

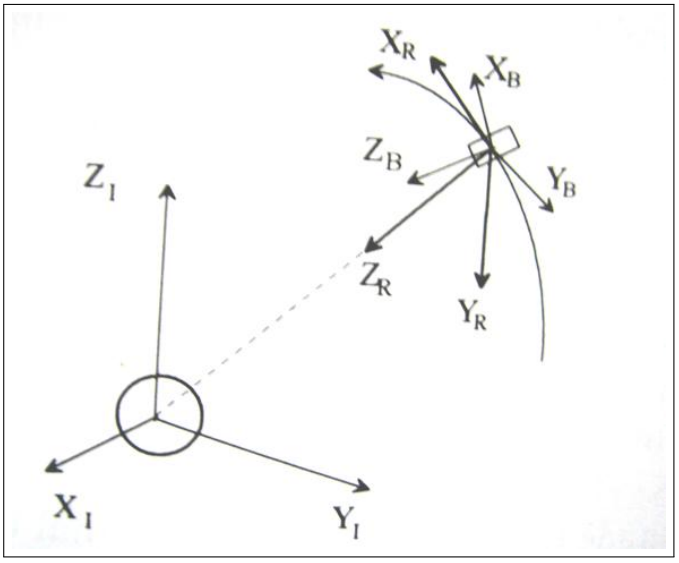

Figure 2.1: Reference Frame

1. Inertial Frame (I)
   $X_I \rightarrow$ First point of Aries
   $Z_I \rightarrow$ Axis of rotation of Earth
   $Y_I \rightarrow Z_I$ x X_I

2. Orbit Reference Frame (R)
   $Z_R \rightarrow$ Towards Earth
   $Y_R \rightarrow$ Opposite to angular momentum of satellite
   $X_R \rightarrow Y_R$ x Z_R

3. Body Frame
   Centered at the mass center and axis perpendicular to faces
   $X_B \rightarrow$ Perpendicular to leading side in the direction of velocity vector
   $Z_B \rightarrow$ Perpendicular to Nadir side towards the earth
   $Y_B \rightarrow Z_B$ x X_B (Perpendicular to antisun side)

4. Earth Centered Earth Fixed frame (ECEF)
   Centered at earth mass center; Fixed to Earth and rotates with it. Two of the axes point to the North Pole and Greenwich meridian.

   A vector is converted from ECI frame to Orbit frame as follows:

$$e_y = -\frac{r \times v}{|r \times v|}$$
$$e_z = -\frac{r}{|r|}$$
$$e_x = e_y \times e_z$$
$$T_{OI} = [e_y\ e_y\ e_y]^T$$
$$v_O = T_{OI} * v_I$$

where, r & v are position and velocity vectors respectively.

Chapter 3

Sensors and Actuators

PRATHAM uses 3 sensors:

- Global Positioning System (GPS) receiver
- 3 axes magnetometer
- 6 Solar cells as Sun sensors

The actuator used is magnetorquer, it is a magnetic coil to produce a magnetic moment that will interact with Earth's magnetic field to produce torque.

3.1 GPS receiver

- The GPS receiver is used for position determination/navigation of the satellite.

Figure 3.1: GPS receiver

- Specifications of the receiver:
  The antenna for receiving signals from the GPS satellites is on the zenith face.

CHARACTERISTICS	SPECIFICATIONS
Box Dimensions	$125 \times 55 \times 40$ mm
Supply Voltage	5 V
Power Consumption	< 2 W (without antenna), < 2.5 W (with antenna)
Receiver	12 channel L1-C/A code SPS
Time to first fix (TTFF) Cold Start (without almanac, time, position)	 90 seconds +/- 30 seconds (typical)
Accuracy (with PDOP < 3.0) Position (Horizontal) Velocity	 10 (2-sigma) meters 0.12 m/s
Dynamics: Velocity	12000 m/s
Position update rate	1 second
Pulse Per Second Pulse Width	 Minimum of 1 ms Maximum of 2 ms
Environmental Characteristics Operation temperature range in Thermovac Storage Temperature Range Vibration Radiation Level	 -25^0 C to $+65^0$ C -40^0 C to $+85^0$ C 15g for 120 seconds in all the three axis Better than 10K rads
PC/ Host Communication Interface Baud Rate Message Formats Start Bits Data Bits Stop Bits Parity Check Flow Control	 RS232 Compatible 9600 Baud Accord's proprietary binary 1 8 2 None None

Table 3.1: GPS Specifications

Use of the GPS receiver-

1. The GPS receiver gives the position and velocity of the satellite in Earth Centered Earth Fixed (ECEF) frame. They are then converted to the Earth Centered Inertial (ECI) coordinates.

ANTENNA ELECTRICAL SPECIFICATIONS	
Frequency Band	1575.42 +/- 10 MHz (GPS L1)
Antenna Gain	+4.5 dBiC nominal @ zenith
Nominal Impedance	50 Ohms
VSWR	<1.9:1
Polarization	Right Hand Circular
Grounding Protection	DC grounded
RF Input	TNC female
LOW NOISE AMPLIFIER SPECIFICATIONS	
Frequency Band (MHz)	1575 +/- 10 MHz (GPS L1)
Amplifier Gain	26 dB (Part no. 1210FW)* 40 dB (Part no. 1213FW)
Nominal Impedance	50 Ohms
Output VSWR	2.0:1 Maximum
Maximum Noise Figure	2.5 dBm maximum
DC voltage	5 to 28 VDC through connector
DC current	25 mA typical , 40 mA Max (13 and 26.5 dB) 40 m A typical, 60 mA MAx (40 dB)
Filtering	Dual Ceramic filters

Table 3.2: GPS antenna Specifications

2. Due to the high power consumption of the GPS, the GPS is not kept on for the entire time. It is switched on so that the position and velocity readings are obtained every 10 minutes. This figure is obtained via simulations done keeping in mind the permissible position error. Intermediate values are propagated using J4-gravity model. (see section on SGP4)

Figure 3.2: GPS Antenna

- Testing of the GPS receiver and antenna-

1. The testing of the GPS was done on the terrace of the Aerospace engineering department.
2. The GPS device was powered on and the data was logged using a serial port for around 6 minutes.
3. The readings for the first 70 seconds were all NULL. After 70 seconds the data was valid and the PDOP value was around 500. Within 20 seconds the PDOP value reduced to around 200.
4. The uncertainty in the X, Y, and Z components was around 1 m. Position error could not be calculated as the true position was not known.

3.2 Three axis magnetometer

The magnetometer is used for attitude determination. It is placed on the lagging face of the satellite.

- Specifications:
  - The 3 axes magnetometer used is the HMR2300. It is a magneto resistive, digital magnetometer.

Figure 3.3: HMR2300 Magnetometer

  - The HMR2300 is chosen because of its favorable characteristics like space grade, space accuracy, space heritage, low weight and size, ease of data communication as seen in the specifications

- Magnetometer Specifications:

CHARACTERISITICS	VALUE	UNIT
Space heritage	Cute 1.7	-
Field range	$\pm$ 2	gauss
Field resolution	70	μ gauss
Weight	98	gram
Size	9.72 x 3.81 x 2.23	cm
Output	Digital (RS 232/RS 485) at 9600 or 19200 baud	-
Error	RSS: 0.52	% FS

Table 3.3: Magnetometer Specifications

- Use of the magnetometer
  - The magnetometer measures the magnetic field in body fixed coordinates.
  - The magnetometer is on right from injection. Readings are used in the detumbling control (B-dot) law
  - The communication of the readings to the microcontroller (μc) is done by the On Board Computer (OBC) team. Their function regarding the magnetometer is data sampling, set-reset and averaging of the data, subject to the constraints of 7 V voltage, 0.03 A current and 0.1 ms time to take the readings
- Sources of error
  - Error due to electronics of the satellite: The magnetometer is surrounded by other satellite electronics, which have a magnetic field of their own. To minimize this error, the magnetometer should be placed as away as possible from the other electronics. Hence the choice of the lagging face, which is relatively free of all other electronics. Also wire routing is done in such a way that wires carrying currents in the opposite direction are placed together. This prevents formation of loops and thus stray moment.
  - Error due to the satellite body: Due to the metallic body of the satellite, there is magnetization error which can change the magnetic field. Coarse experiments done by covering the magnetometer with an aluminium box, give an error in the magnetic field of 2 mgauss.
  - Mounting error: There will always be a misalignment between the magnetometer axes and the satellite body axes. Tolerances are given to the integrations team for the same.
  - Error due to temperature variation: Temperature varies from -10 to 60 degree Celsius. This introduces a scaling error, the maximum value of which is 2.1
  - Drift error: The magnetic field reading at the same point varies with time. This is known as drift. Experiments were performed, which put a value to the drift as $\sim$ 2.5 μ gauss/s.

Characteristic	Conditions	Min	Typ	Max	Unit
Supply Voltage	Pin 9 referenced to pin 5	6.5		15	Volts
Supply Current	Vsupply=15V, with S/R=ON		27	35	mA
Operating Temperature	Ambient	-40		85	°C
Storage Temperature	Ambient, unbiased	-55		125	°C
Field Range	Full scale (FS) - total applied field	-2		+2	Gauss
Linearity Error	Best fit straight line ±1 Gauss (at 25°C) ±2 Gauss		0.1 1	0.5 2	%FS
Hysteresis Error	3 sweeps across ±2 Gauss @ 25°C		0.01	0.02	%FS
Repeatability Error	3 sweeps across ±2 Gauss @ 25°C		0.05	0.10	%FS
Gain Error	Applied field for zero reading		0.05	0.10	%FS
Offset Error	Applied field for zero reading		0.01	0.03	%FS
Accuracy	RSS of all errors ±1 Gauss (at 25°C) ±2 Gauss		0.12 1	0.52 2	%FS
Resolution	Applied field to change output	67			µGauss
Temperature Effect	Coefficient of gain Coefficient of offset (with S/R ON)		-600 ±114		ppm/°C
Power Supply Effect	From 6 -15V with 1G applied field		150		ppm/V
Vibration (operating)	5 to 10Hz for 2 hours 10Hz to 2kHz for 30 min.		10 2.0		mm g force
Max. Exposed Field	No perming effect on zero reading			10	Gauss
Weight	Board only In Aluminum Enclosure - extended - flush base		28 98 94		grams

Figure 3.4: Magnetometer Specifications

  - Bias and random error: The maximum bias is $3e^{-4}$ gauss. The maximum random error is $52e^{-4}$ gauss.
  - Sudden changes in magnetic field (of the factors of 4 and 5) will be taken care of by putting checks on the OBC.

- Calibration of the Magnetometer
  - Calibration was carried out using a Helmoltz coil setup. The magnetometer was placed on a platform with one of its axes aligned with the axis of the coils and a current was passed through the coils to generate a known magnetic field.
  - The field was then recorded by the magnetometer and after the field value settled, a time averaged reading was recorded and compared to the known value.
  - The field was varied from -1 to 1 Gauss.
  - The calibration curve along all the axes was observed to be linear.

- Results
  - The result for X axis is as shown below (squared correlation coefficient (R^2) = 1 RMS error: 8.9x10^{-4})

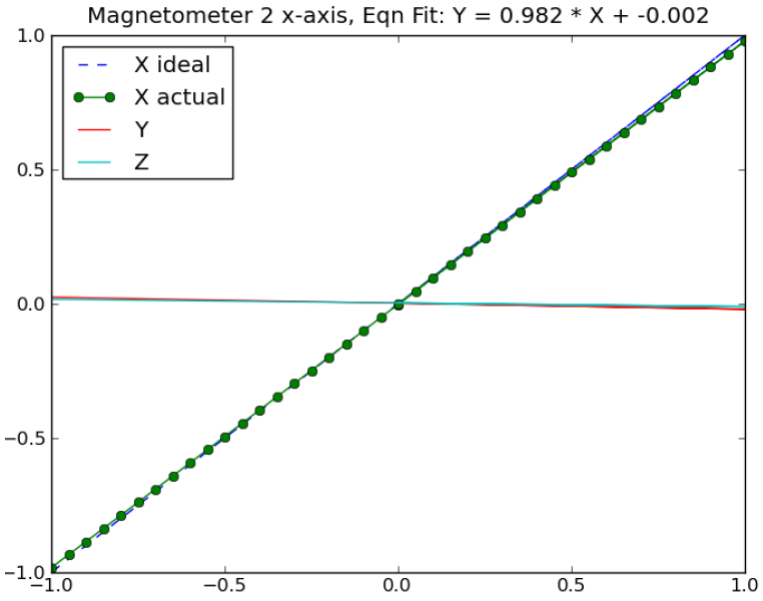

Figure 3.5: Calibration along x-axis

  - The result for Y axis is as shown below (R^2 = 1 RMS error: 9.5x10^{-4})

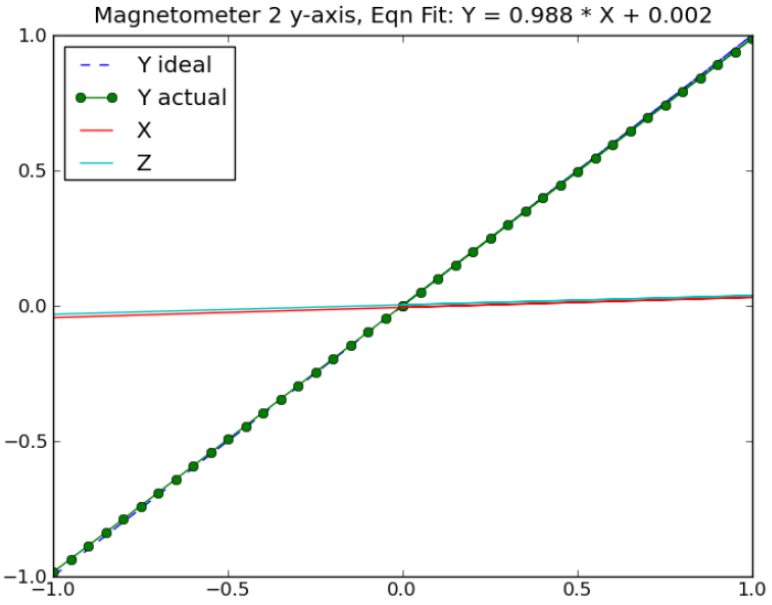

Figure 3.6: Calibration along y-axis

– The result for Z axis is as shown below (R^2 = 1 RMS error: 3.6x10^{-4})

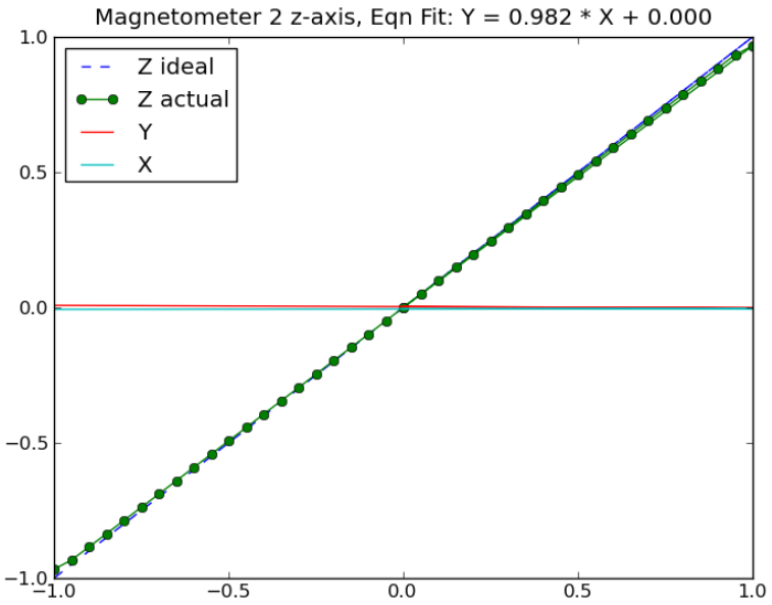

Figure 3.7: Calibration along z-axis

3.3 Sun sensors (SS)

* Directional solar cells are used as sun sensors. 6 solar cells are placed on the face centers. The SS are used in attitude determination. The solar cells give an output depending on the angle made by the sensor normal to the sun vector. The lesser the angle, the more is the output.
* Specifications of the receiver:

SL. NO.	DEVICE PARAMETERS	SPECIFICATIONS
1.	Type of detector :	Silicon planar diffused 'n on p' junction
2.	Size:	5mm± 0.05mm x 5mm± 0.05mm
3.	Active region :	4mm±0.02mm x 4.5mm±0.02mm
4.	Responsivity:	Responsivity of the photosensor shall be a minimum of 35mA/cm^2 (AMO) at 25^{0}C
5.	Wafer Thickness:	0.35 to 0.40mm
6.	Resistivity:	10±3 ohm-cm
7.	Short circuit current, I_{sc}:	>35 mA/cm^2 at one solar constant
8.	Dark Current, I_d:	max. 50nA at V_R = 2V (at 23^0 C ± 3^{0}C)
9.	Reverse break down voltage:	5V minimum
10	Shunt resistance, R_{sh}:	>1MΩ in short circuit mode
11	Series resistance, R_s:	Less than 10Ω in short circuit mode
12	Junction capacitance, C_j:	< 8nf typical at V_R = 2V < 15 nf typical at V = 0V
13	Variation in the dark current w.r.t temperature:	Not more than double for every 5^{0}C temperature increase
14	Operating temperature:	-85^{0}C to +85^{0}C
15	Storage temperature :	-100^{0}C to +100^{0}C
16	Anti reflection coating:	Compatible to apply the adhesive 'DC 93500' and meet the responsivity requirement specified
17	Uniformity:	Variation in I_{sc} not more than ±5%
18	Radiation resistance:	% degradation of responsivity not more than 12.5% for an electron fluence of 7x10^{14}e/cm^2 of 1 MeV
19	UV degradation:	not more than 2% for radiation of 1250 equivalent sun hours at a minimum vaccum of 10^{-5} Torr

Figure 3.8: Sun Sensor Specifications

– **SS electronics**

  * A simple current to voltage convertor followed by a 10-bit ADC is used to obtain digital values of voltage readings from each SS.

– **Use of the SS**

  * The solar cells give an output depending on the angle made by the sensor normal to the sun vector. The lesser the angle, the more is the output. The relation is

approximately

$$I = I_0 cos\theta \tag{3.1}$$

where I_0 is the intensity at 0 angle.

* The voltage output is controlled by the SS board circuitry.
* The reconstruction from the SS readings is explained in the simulations chapter.
* In the eclipse part, the readings from all SS are expected to be approximately 0.
* The SS aren't on all the time. They are switched off during the detumbling phase. They work in tandem with the magnetometer only in the nominal phase.

3.4 Magnetorquers

– 3 orthogonal magnetorquers form the actuator system of the satellite.

– Torquer specifications:

Sr. No.	Parameter	Value	Unit
1.	21x21	Cute 1.7	cm^2
2.	Resistance	$\sim$ 15.6 2	Ohm
3.	Inductance	$\sim \mu$	Henry
4.	Max moment	0.95	Am^2
5.	No. of turns	40	-
6.	PWM resolution	16	bits

Table 3.4: Magnetorquer Specifications

Chapter 4

Simulations

4.1 Overview

- The simulations involve the satellite mechanics and dynamics, the satellite environment, the sensor models, the onboard computations (involving navigation and attitude determination), the control law and the torque actuation.
- Block diagram:

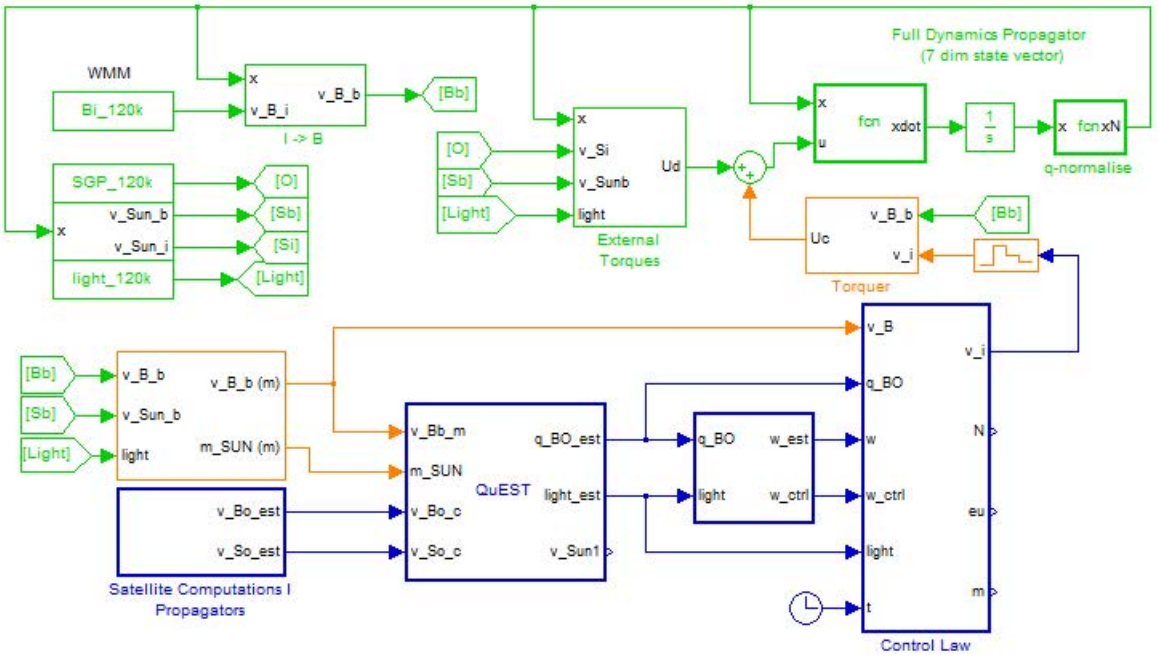

Figure 4.1: ADCS Simulation Block

The green blocks are the environment simulation blocks, which run at a time step of 0.1 sec.
The orange blocks are the hardware blocks, which simulate the noise of the sensors. The output of the hardware blocks is similar to what would be really obtained on board.
The blue blocks are the On Board Calculation (OBC) blocks which evaluate once every frame (2 sec), and hold that value until the next evaluation.

*In All block diagrams, WMM stands for World Magnetic Model 2005, which is now replaced with IGRF-11 13^{th} order for Environment and IGRF-11 8^{th} order for On-board.

Signal flow in a nutshell:

- The SGP4 orbit propagator is the 1st block to evaluate, and runs independently of other blocks. It gives the position vector in ECI frame (O). The Sun model is also independent of any other blocks and depends only on time. It outputs the sun vector (S). Magnetic field (B) in ECI frame is obtained from position vector using IGRF -11 13^{th} order model. All these environmental models run offline.
- Eclipse model is based on O and S and gives the light signal (a Boolean indicating light/dark).
- Disturbance torques are calculated from S, B, O, and the previous state vector (x). These, along with the control torque, are input to the attitude dynamics propagator which outputs the next state (x). x is the attitude quaternion and rate (of body frame with respect to the ECI frame).
- Real S, B, body frame and O go to hardware blocks which output the measured vectors (position and velocity vector readings from the GPS receiver and the magnetic field vector readings (BB) from the magnetometer) and the 6 sun sensor readings. The SS algorithm extracts the sun vector in the body frame (SB). It also estimates whether the satellite is in the light or eclipse phase.
- The GPS gives the position and velocity vectors at only 10 min intervals. In between the position and velocity are propagated onboard using a simple J2 propagator, fed with initial conditions from the GPS receiver. The position readings are used to calculate the orbit frame magnetic field vector (using IGRF-11 8th order model) (B_O) and the orbit frame sun vector (S_O) on board using on board models.
- The Quaternion Estimation (QuEST) is used to estimate the orbit to body frame quaternion (q_{BO}) (desired to be kept as small as possible within $\pm$ 10 degrees) from $B_B, B_O, S_B, S_O, q_{BO}$ is differentiated to find the rate of the satellite with respect to the orbit frame, expressed in body frame (w_{BOB}).
- These are then used to calculate control torque via the control law.
- The required torque is then applied by the actuator (magnetotorquer). This torque along with the disturbance torques is applied to the real dynamics propagator for state propagation.

4.2 Frames of reference

- Inertial Frame (I)
  X $\rightarrow$ First point of Aries
  Z $\rightarrow$ Axis of rotation of Earth
  Y $\rightarrow$ Z $\times$ X
- Orbit Reference Frame (R)
  X $\rightarrow$ Y $\times$ Z

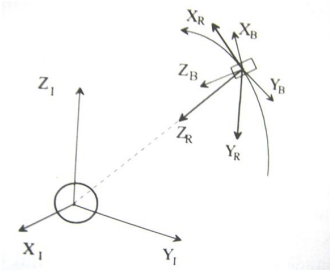

Figure 4.2: Reference Frames

Z $\rightarrow$ Towards Earth
Y $\rightarrow$ Opposite to angular momentum of satellite

- Body Frame
  Along the geometric body axes
- Earth Centered Earth Fixed frame (ECEF)
  Fixed to Earth and rotates with it. Two of the axes point to the North Pole and Greenwich meridian.
  A vector is converted from ECI to Orbit as follows:

$$\begin{cases} e_y = -(r \times v)/|r \times v| \\ e_z = -r/|r| \\ e_x = e_y \times e_z \\ T_{OI} = [e_x e_y e_z]^T \\ v_O = T_O I * v_I \end{cases} \tag{4.1}$$

4.3 Environmental models and real propagators

- Real Dynamics propagator

$$\Omega = \begin{bmatrix} 0 & w(3) & -w(2) & w(1) \\ -w(3) & 0 & w(1) & w(2) \\ w(2) & -w(1) & 0 & w(3) \\ -w(1) & -w(2) & -w(3) & 0 \end{bmatrix} \tag{4.2}$$

$$\begin{cases} \dot{q} = 0.5\Omega q \\ \dot{w} = I^{-1}(u - w \times Iw) \end{cases} \tag{4.3}$$

- Real Orbit propagation: SGP4 model

  - The Small Gravitational Perturbation Model is a standard gravity model for the earth.
  - It is a sophisticated model which iteratively calculates the earth's gravity at any point by including effects like J2, J3, secular effects of gravitation, periodic effects of gravitation, short term perturbations.
  - The inputs are the orbital elements of the satellite orbit (sun synchronous, 500 to 800 km altitude) in the form of a Two Line Element (TLE).
  - The output is the ECI position and velocity vector.

- Sun model
  - The sun model takes as input the time elapsed since the latest vernal equinox.
  - It gives as output the ECI sun vector. Calculation is shown below:

t = days since the equinox

$$\begin{cases} \lambda = 2\pi \frac{t}{365.256363} \\ \varepsilon = \frac{23.5\pi}{180} \\ sin(\delta) = sin(\varepsilon)sin(\lambda) \\ tan(\alpha) = \frac{cos(\varepsilon)sin(\lambda)}{cos(\delta)} \\ x = cos(\delta)cos(\alpha) \\ y = cos(\delta)sin(\alpha) \\ z = sin(\delta) \\ v_{Sun_i} = [x; y; z]; \end{cases} \tag{4.4}$$

    where r and v are the position and velocity vectors respectively.

- True Magnetic field model: IGRF-11 O-13
  - International Geomagnetic Reference Field 2011 (IGRF -11) model is used.
  - It calculates the geomagnetic field vector in the ECI frame. It models the earth's magnetism as a magnet with the desired order of polarity (dipole, quadrapole, octapole,etc.). Here a 13th order model is used.
  - The input is the position of the satellite in the ECI frame.

- Light model
  - It says whether the satellite is in light or eclipse region (shadow of the earth on the satellite).
  - The satellite is assumed to be a point mass. However the Sun and the earth are assumed to finite size spheres.
  - When in the umbra or penumbra of the earth, the satellite is in eclipse phase. The sun sensors give no readings. Otherwise the satellite is in light.
  - The input is the position of the satellite. The equations for calculation are as follows:

$$\begin{cases} r_{umbra} = \frac{r_0 R_e}{(R_s - R_e)} \\ r_{penumbra} = \frac{r_0 R_e}{(R_s + R_e)} \\ \alpha = asin(\frac{R_e}{r_{umbra}}) \\ \beta = asin(\frac{R_e}{r_{penumbra}}) \\ \theta = acos(\frac{x.v_s}{|x|}) \\ p_u = acos(\frac{x + r_{umbra}.v_s}{|x + R_{umbra}|}) \\ p_p = acos(\frac{x - R_{penumbra}).v_s}{|x - R_{penumbra}|}) \\ if \theta \geq \frac{pi}{2} + \alpha \&\& p_u \leq \alpha \\ light = 0; \\ else \\ light = 1 \end{cases} \tag{4.5}$$

4.4 Disturbance torque models

– Gravity Gradient torque:

$$\tau_{GG} = \frac{3\mu}{|r_B|^5} r_B \times I r_B \tag{4.6}$$

where r_B = position vector in body frame,
I = inertia matrix

– Solar drag force:
Solar radiation exerts a drag force on satellite and thus a corresponding torque.

$$F_{Solar} = -A_P C_a P_{flux} \hat{v_{SB}} * light \tag{4.7}$$

– Aerodynamic drag force:

$$F_{aero} = -0.5 A_P C_D \rho |v_B|^2 v_B \tag{4.8}$$

Torque exerted = force crossed with vector from center of mass to center of pressure.
where A_p = projection area,
C_D = drag coefficients,
v_B = position vector in body frame,
ρ = atmospheric density.

4.5 Sensor modeling

– GPS modeling

* The inputs are the position and velocity vectors from the SGP4 model.
* Random errors in the range as specified in the datasheet are added to the input to give the sensor readings.

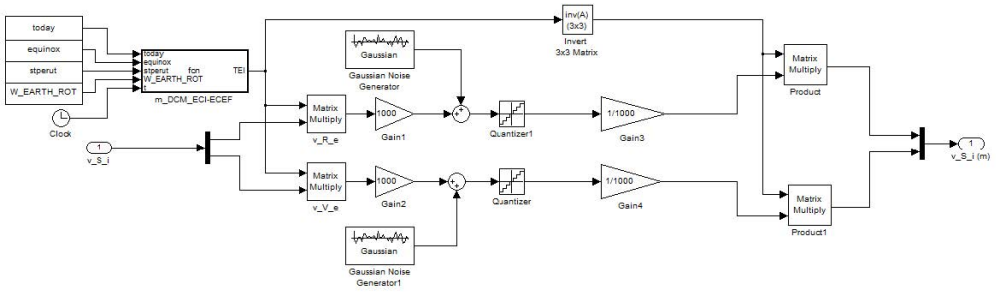

Figure 4.3: GPS modeling

– Magnetometer modeling
  * The input is the geomagnetic field vector from the IGRF environmental model.
  * The RSS error is simply added to the above. Additional bias is also included for robustness.

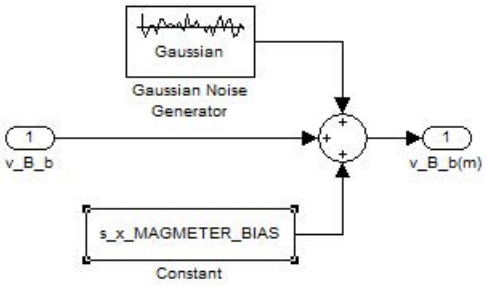

Figure 4.4: Magnetometer Modeling

– SS modeling
  * The input to the SS model is the sun vector in the body frame.
  * The model involves adding random error, saturation, ADC gains to the sensor output (a measure of the angle between the sensor normal and the sun vector) to give the SS readings.
  * The output of all the 6 SS is theoretically 0 in the eclipse region. But in the sensor block, noise does not allow it to be exactly zero.

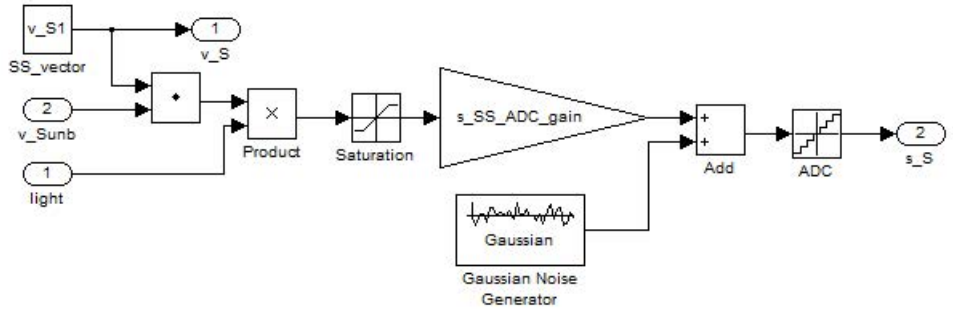

Figure 4.5: Sun Sensor Modeling

4.6 Onboard computations

– Orbit propagation/Navigation

  * This model propagates the ECI position and velocity (i.e. the orbit basically) of the satellite between two successive GPS readings. The GPS readings serve as the initial conditions every 10 minutes. (The resetting of the initial conditions is done by the pulse generator in the simulations).
  * The main calculation is that of the earth's acceleration due to gravity at any point. It is integrated successively to get velocity and the position.
  * The acceleration due to gravity g is calculated by employing a J2 model of the earth's gravity. It is important to incorporate J2 because this is the effect responsible for sun synchronous orbits.
  * The model equations are:

$$\begin{cases} V = \frac{\mu}{r}[1 - \sum_{n=1}^{\infty} \frac{a}{r}^{2n} J_{2n} P_{2n}(cos\theta)] \\ V_{J2} = -\frac{\mu}{r}[1 - \frac{J_2}{2}(\frac{a^2}{r^2})^2(3cos^2\theta - 1)] \\ g = -\nabla V_{J2} \\ g_x = -\frac{\mu x}{r^3}(1 + \frac{3}{2}J_2\frac{a^2}{r^2} - \frac{15}{2}J_2\frac{a^2z^2}{r^4}) \\ g_y = -\frac{\mu y}{r^3}(1 + \frac{3}{2}J_2\frac{a^2}{r^2} - \frac{15}{2}J_2\frac{a^2z^2}{r^4}) \\ g_z = -\frac{\mu z}{r^3}(1 + \frac{9}{2}J_2\frac{a^2}{r^2} - \frac{15}{2}J_2\frac{a^2z^2}{r^4}) \end{cases} \tag{4.9}$$

– Calculation of sun vector and magnetic field vector in the orbit frame

  * The position vector obtained from the orbit propagator is used as input to calculate the sun vector and magnetic field vector in the orbit frame.

  - The sun model described above is used for calculating the sun vector onboard too. The time elapsed from vernal equinox is required as the input
  - The magnetic field vector is calculated using the IGRF-11 model of order 8.

- Estimation of light/eclipse, reconstruction of the sun vector and QuEst
  - The first step is to estimate if the satellite is in light or eclipse. This is done by the 6 SS measurements. If all the SS readings are < some threshold (i.e. cos(half FOV)*max. SS gain), the satellite is in eclipse. Otherwise it is in light. If the satellite is in light, we use the 6 SS readings to reconstruct the sun vector in the body frame and then use the 4 vectors (measured and propagated magnetic filed vector and sun vector) to obtain quaternion using QuEST.
    Sun vector reconstruction: let a1, a2, a3 be three SS normal vectors that see the sun. Their corresponding outputs be V1, V2, V3 and angles with the sun vector v be $\theta_1, \theta_2, \theta_3$,
    then

$$\begin{cases} a_1^T v = cos(\theta_1) = V_1/V_0 = kV_1 \\ thus, \\ Av = kV \\ v = kA^{-1}V \end{cases} \tag{4.10}$$

    Now normalize v to eliminate k: $\hat{v} = (A^{-1}V/|A^{-1}V|)$ For choosing the 3 SS, sort them according to their outputs and choose the top three, while keeping a check to not include anti-parallel sunsensors.
  - The Quaternion Estimation (QuEST) algorithm is used to estimate the attitude. The attitude is estimated by the orbit frame to body frame quaternion, qBO. The QuEST algorithm requires two non parallel reference vectors in the orbit frame and two non parallel measurement vectors in the body frame. The sun vector and magnetic field vectors in the respective frame are used for the QuEST.
    If the satellite is in eclipse, the quaternion cannot be estimated. It is simply output as [0;0;0;1].
  - Calculation of wBO from qBO:

$$\omega_{BOB} = 2(\eta I_{3\times 3} - \eta\varepsilon^x + \varepsilon\varepsilon^T)\dot{\varepsilon}/\eta \tag{4.11}$$

    Since just after eclipse, the filtered w readings are incorrect for a few seconds, we multiply it by a ω_{ctrl} pulse, which is 1 everywhere except 300 seconds after light region is entered.
    - filter w using I order low pass filter with time constant = 60 s
    - generate ω_{ctrl} pulse to delay control by w (reason discussed in control strategy later)

    By this logic, ω_{ctrl} is is 0 for 300 s after light region begins, and 1 else.

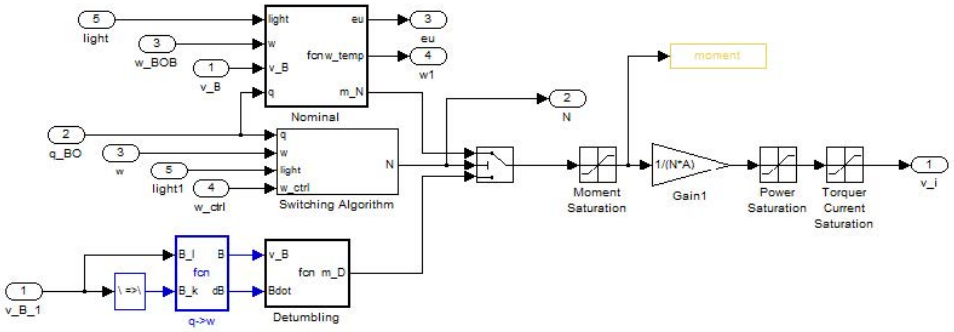

Figure 4.6: Control Law simulation block

– Control law

  * Nominal Controller :

$$m = K_p \frac{\theta}{|B|^2} + K_d \frac{\omega_{BO}}{|B|^2} \tag{4.12}$$

  where $\theta = 2q_v q_0$
  m_n = m × B
  Also,
  $K_p = 1/(T^2\zeta^2)$
  $K_d = 2I/T$
  where ζ and T are chosen to be 1.15 and 0.125* T_{orbit} respectively
  and m_n = control moment,
  q_v=quaternion vector part,
  q_0 = scalar part,
  B = magnetic field in body frame.

  * Detumbling Controller :
  B dot controller is used. Magnetic moment in detumbling is calculated as:

$$m_d = -KB_0\Big(\frac{\dot{B}}{|B|}\Big) \tag{4.13}$$

  where K = 4×10^4, is a constant gain.

  * Switching:

  Switching strategy is defined as follows:

  1. For the first 2000 s, run detumbling mode.
  2. After initial detumbling (and also in general), switching to nominal will occur if
     a) The angular rates drop below a certain threshold (4e-8 rad/s). But since the rates are estimated from the quaternions, there can be sudden peaks and drops in the rates due to noise. Therefore, a window of 60 seconds has been

defined such that if the rates are consecutively low for this duration, then switch to nominal.
b) The satellite is in light region.
c) The satellite was in light 300 seconds before. This is done, so that the switching does not occur in the penumbra region of eclipse.

3. Switching to detumbling mode will occur if
a) The angular rates increase over a threshold (8e-8 rad/s) for a window of 60 seconds as with the case of nominal. There is no switching between 4e-8 and 8e-8. The threshold for the rates have been decided by observing the angular rates as they stabilize from detumbling to nominal.
b) A check time of 10,000 seconds is kept for switching from nominal to detumbling.

4. In order for the switching to take place from detumbling to nominal, estimated angular rates are needed. The angular rates are estimated using the QuEst algorithm which requires the position and velocity of the satellite. Hence, GPS has to be on for the switching to take place. GPS is switched on when
a) The average of norm of magnetic moment decreases below 0.04 N/m. For initial switching, if the magnetic moment does not fall below the threshold, switching will still take place if time elapsed is more than 6 complete orbits. The time has been decided by observing the initial switching for worst case scenario of initial rates of 12 deg/s along the three axes.
b) GPS is kept switched off in eclipse region and is switched on 150 seconds before light region. The time of eclipse is estimated beforehand from the altitude and the orbit geometry.

4.7 OILS

In order to verify the C-code of the control algorithm which will be part of the overall flight code, the sensor data are simulated from the environment data without noise and given as an input to the OBC C code at a time step of 2 seconds. Noise is not added since it is in open loop. All the switching conditions of GPS starting and detumbing to nominal are verified. The outputs of current and quaternion are also verified from the data of the closed loop matlab model. The currents are seen to stabilize hence verifying the C code.

The setup for OILS is described pictorially as follows

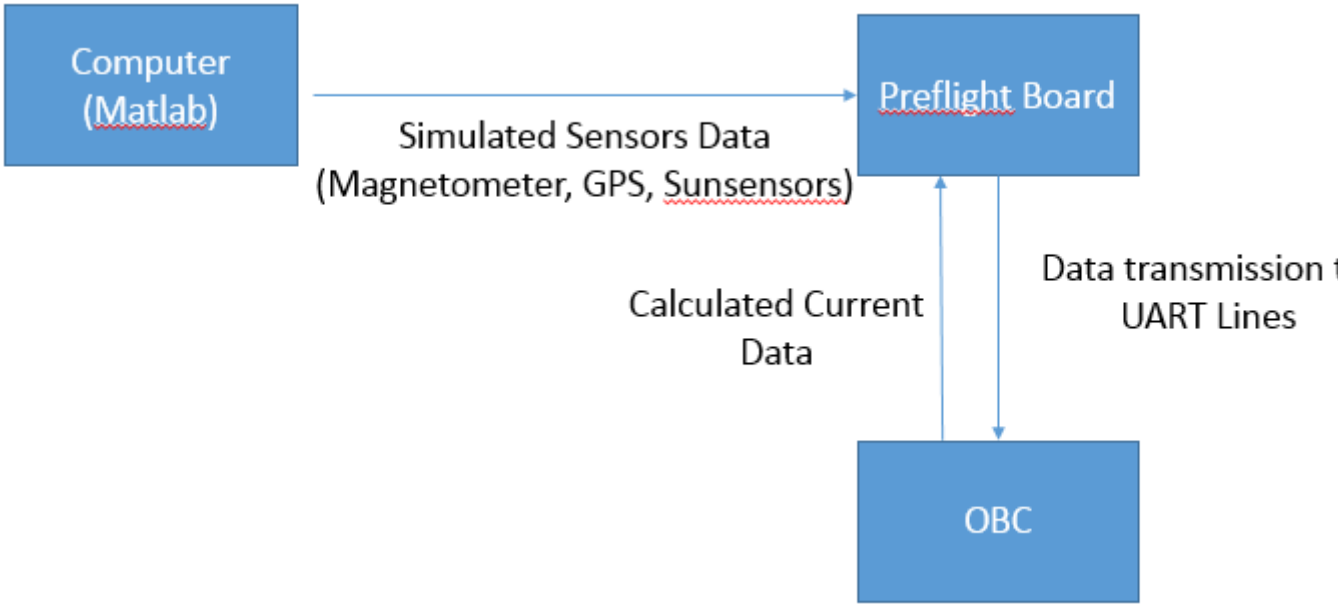

Figure 4.7: Detumbling current from C code

The currents from the C code are plotted below

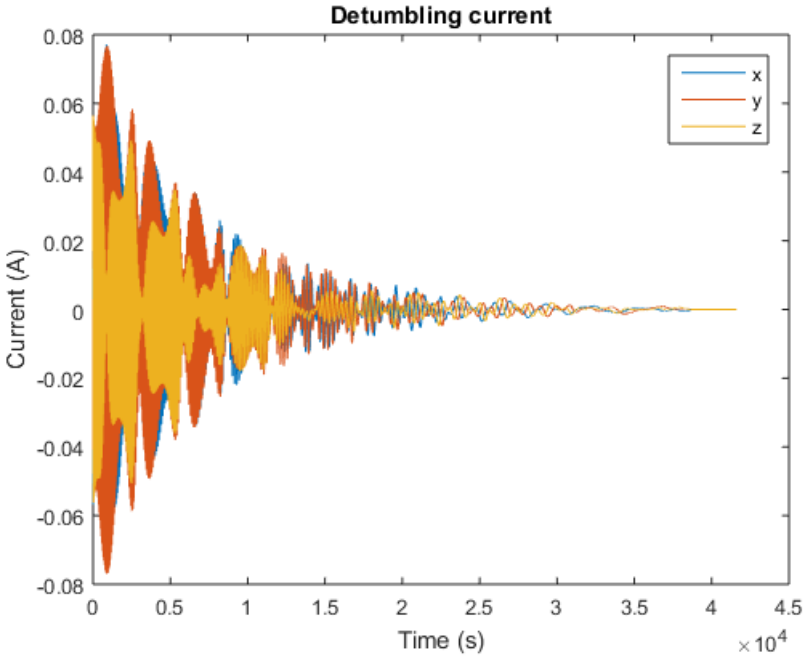

Figure 4.8: Detumbling current from C code

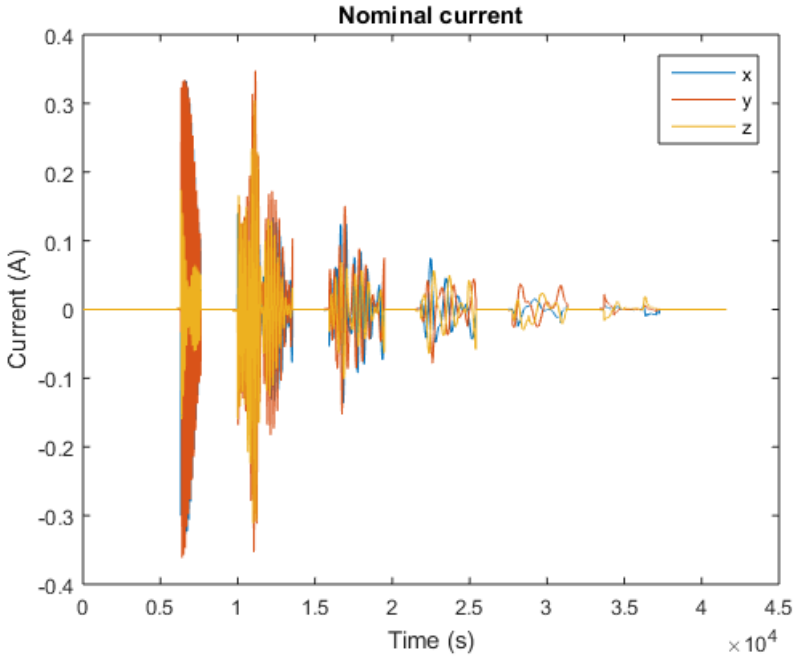

Figure 4.9: Nominal current from C code

Chapter 5

Simulation Results

Latest results show that satellite attitude is controlled well within the bounds imposed by the payload and communication teams, even if initial conditions are large for all the four altitudes that the simulations were carried out-500 km, 600 km, 700 km, 800 km. Unless stated otherwise, the results are for 500 km.

5.1 Case 1: Nominal launch conditions:

Initial Angular rates: [5,5,5] deg/s along the X,Y,Z body axes respectively
Initial Euler angles: 20^0 roll, 140^0 pitch, 80^0 yaw

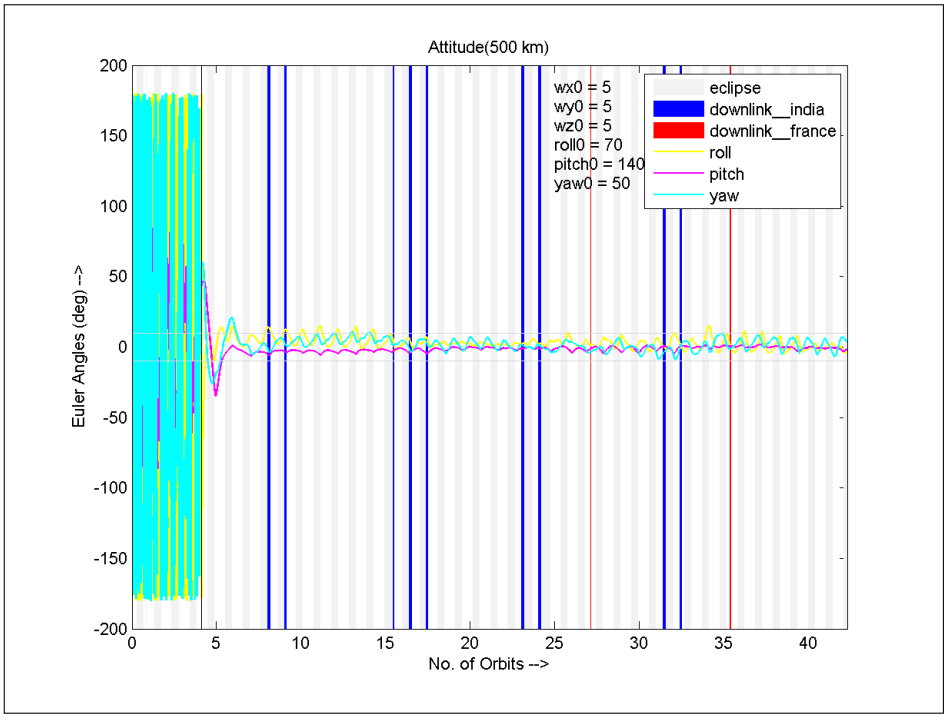

Figure 5.1: Euler angles

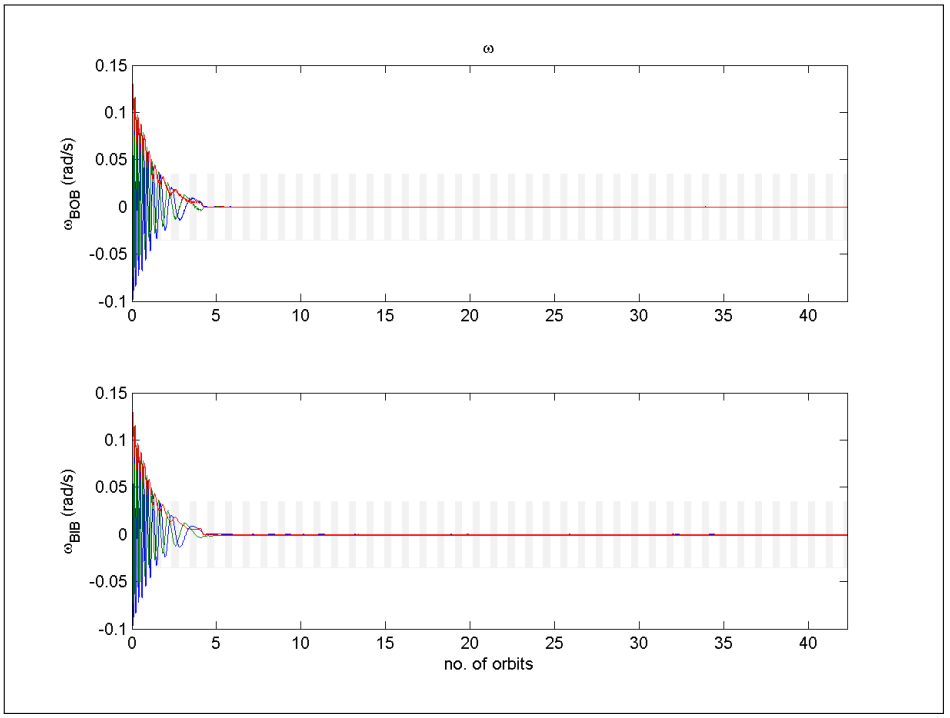

Figure 5.2: Rate of orbital frame/inertial frame w.r.t body frame expressed in body frame

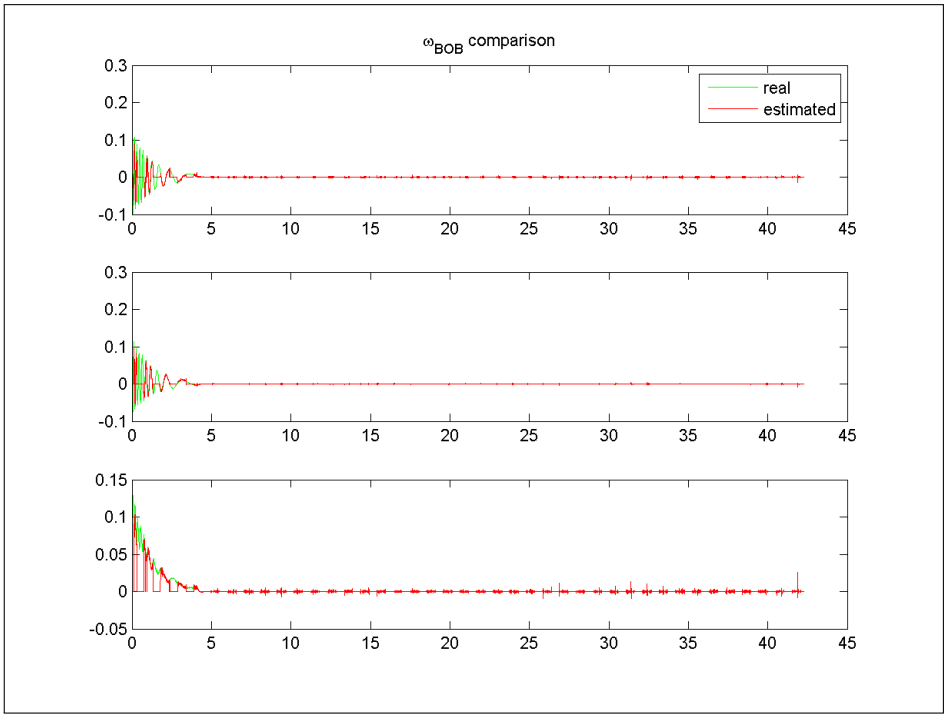

Figure 5.3: Rate of orbital frame w.r.t body frame expressed in body frame, estimated v/s real

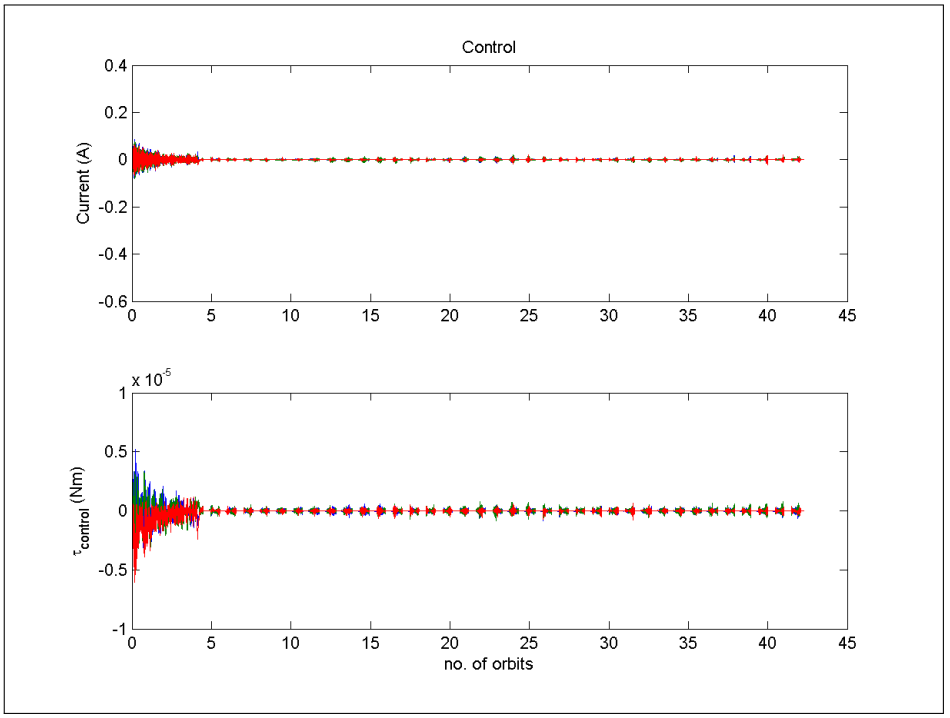

Figure 5.4: Control current and torque

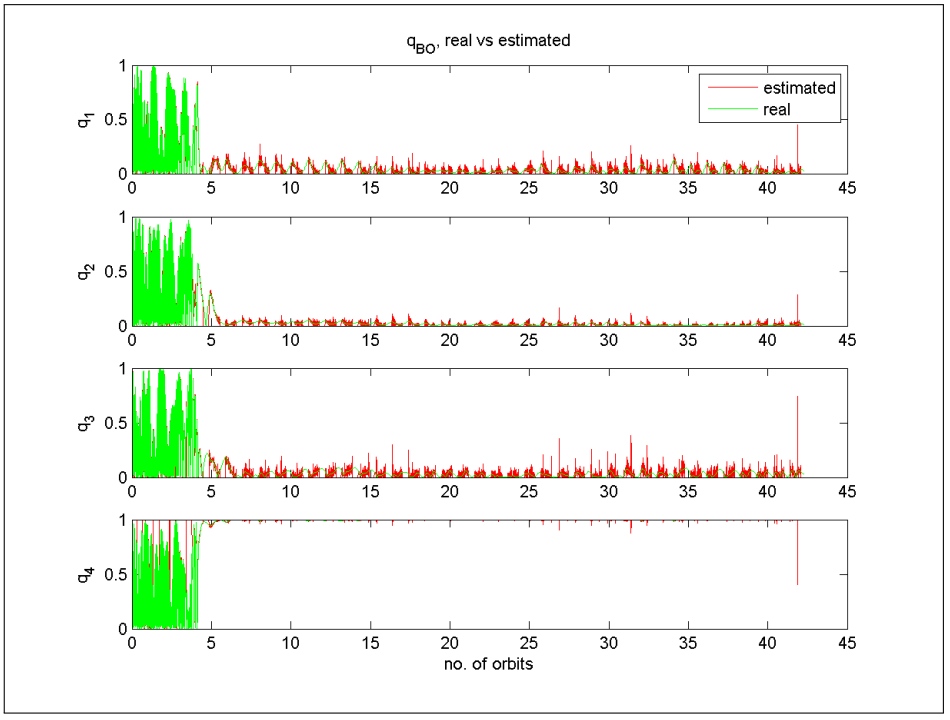

Figure 5.5: Quaternion of orbital frame w.r.t body frame

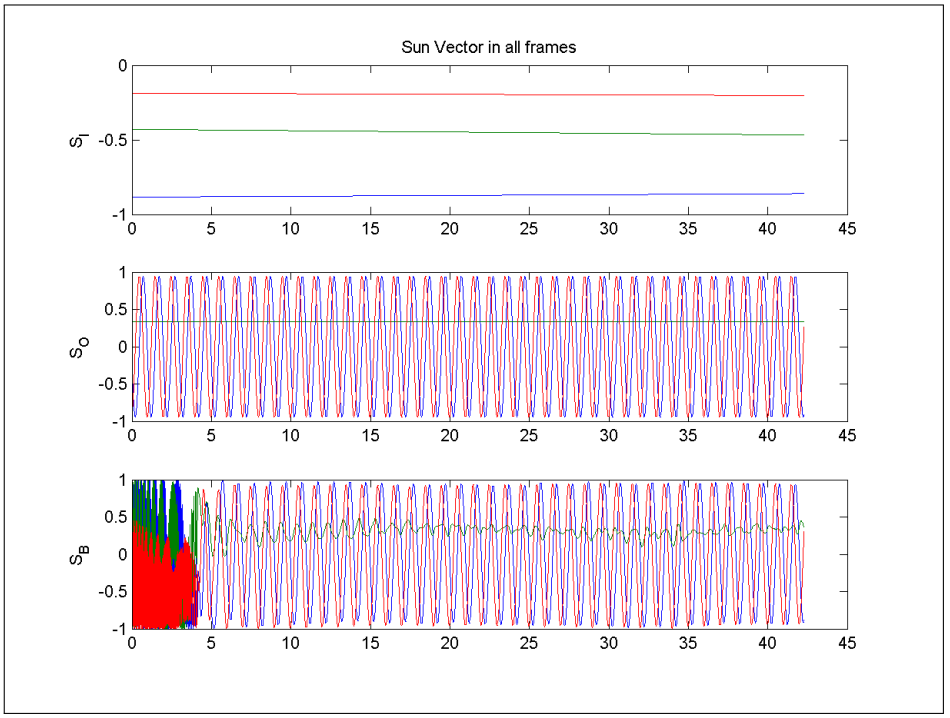

Figure 5.6: Sun vector expressed in different frames

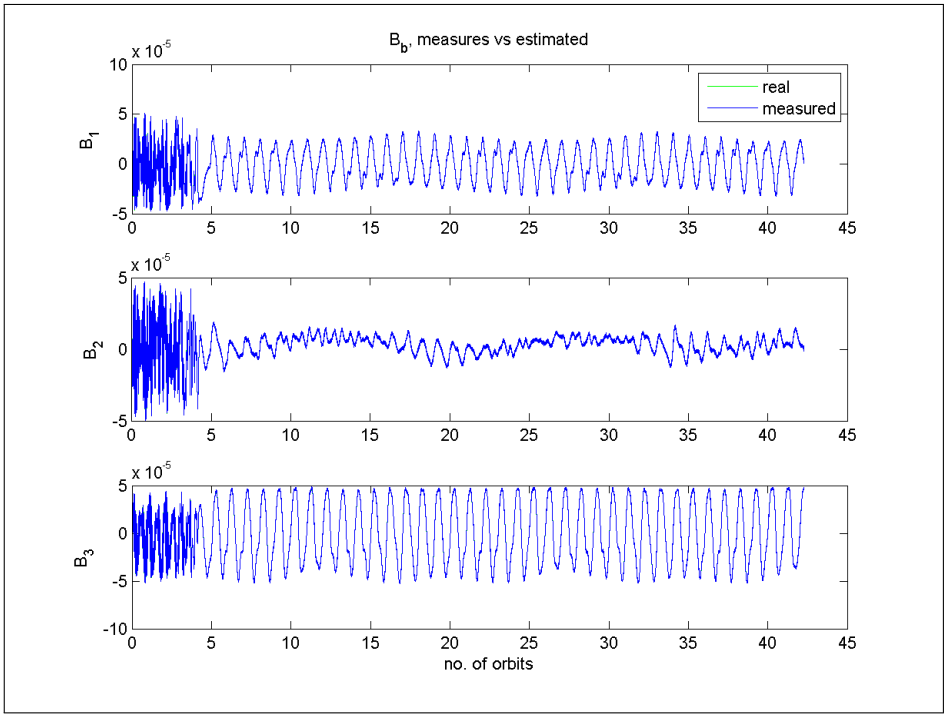

Figure 5.7: Magnetic field measured v/s estimated

5.2 Case 2: High initial rates:

Initial Angular rates: [12, 12, 12] deg/s along the X,Y,Z body axes respectively
Initial Euler angles: 20^0 roll, 140^0 pitch, 80^0 yaw

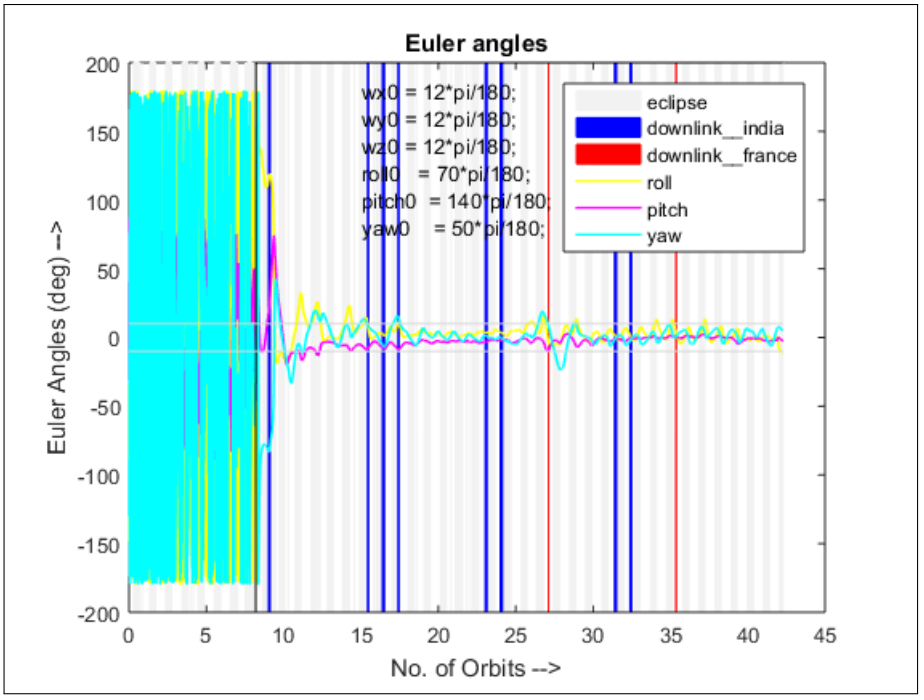

Figure 5.8: Euler angles

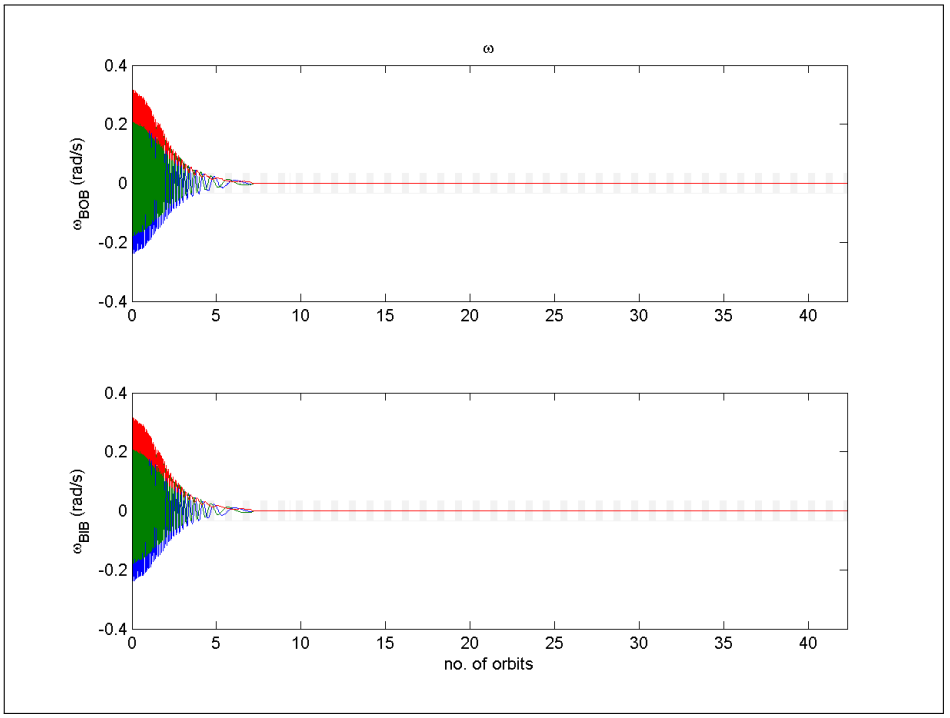

Figure 5.9: Rate of orbital frame/inertial frame w.r.t body frame expressed in body frame

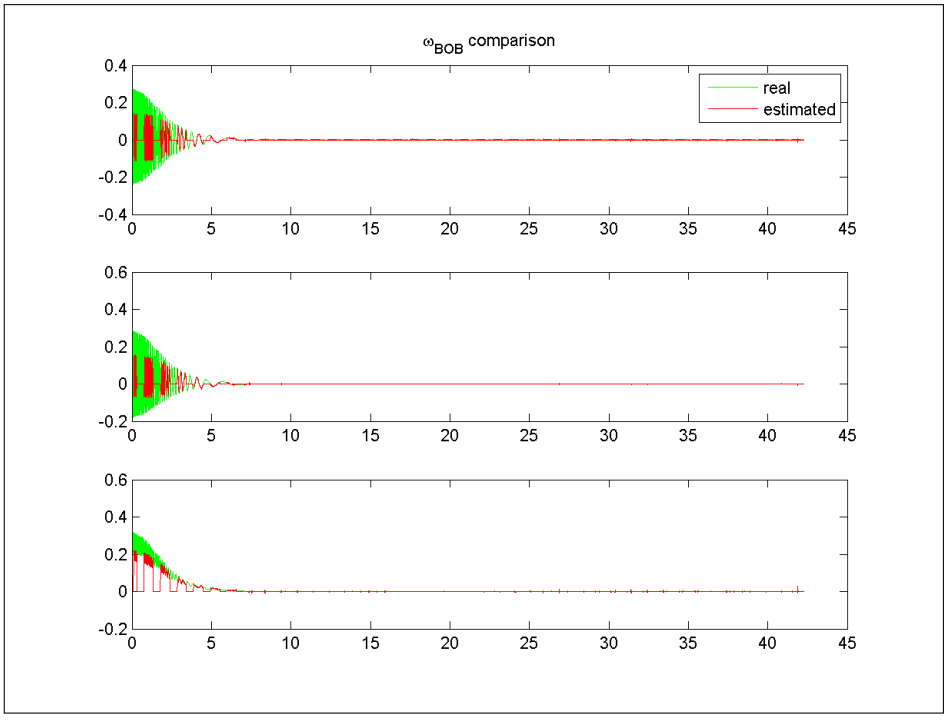

Figure 5.10: Rate of orbital frame w.r.t body frame expressed in body frame, estimated v/s real

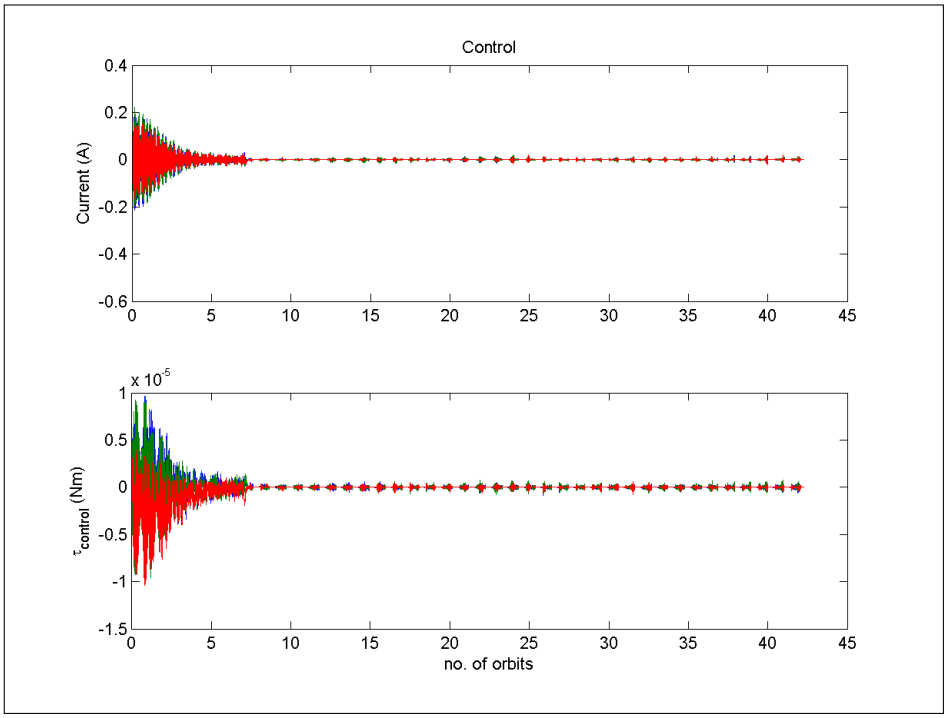

Figure 5.11: Control current and torque

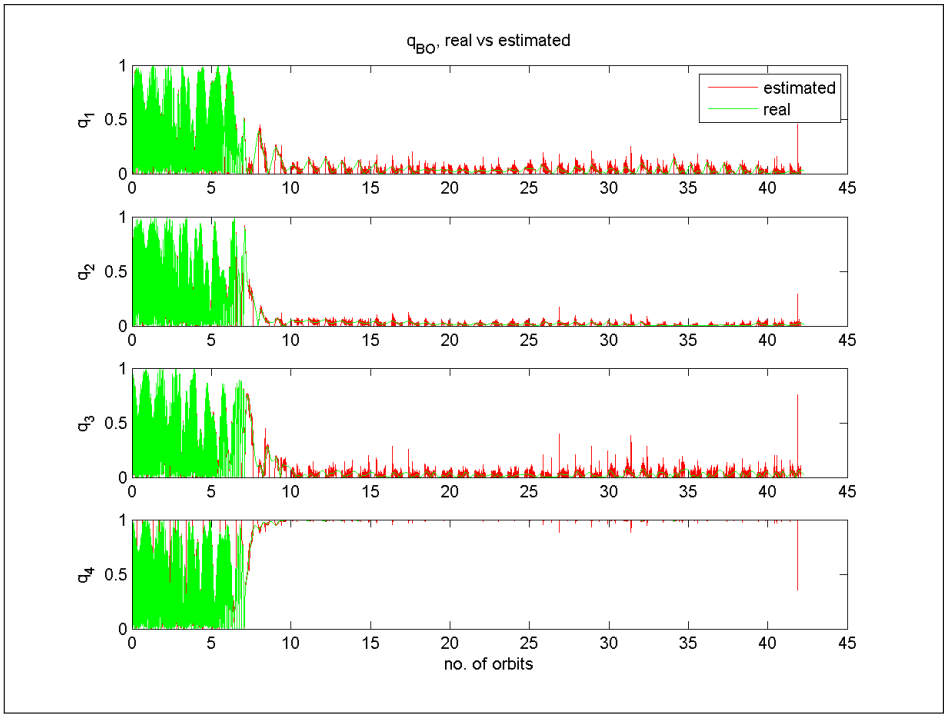

Figure 5.12: Quaternion of orbital frame w.r.t body frame

5.3 Inertia variations:

Case 1: The whole inertia matrix is scaled by a factor of 1.5.
Initial Angular rates: [5 5 5] deg/s along the X,Y and Z body axes respectively.
Initial Euler angles: 20^0 roll, 140^0 pitch, 80^0 yaw

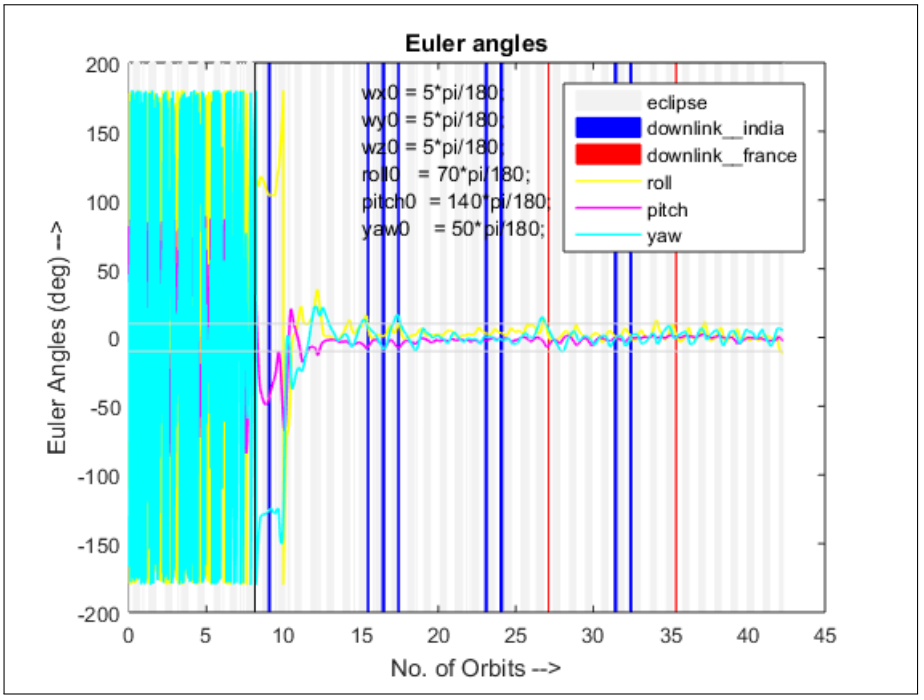

Figure 5.13: Euler angles

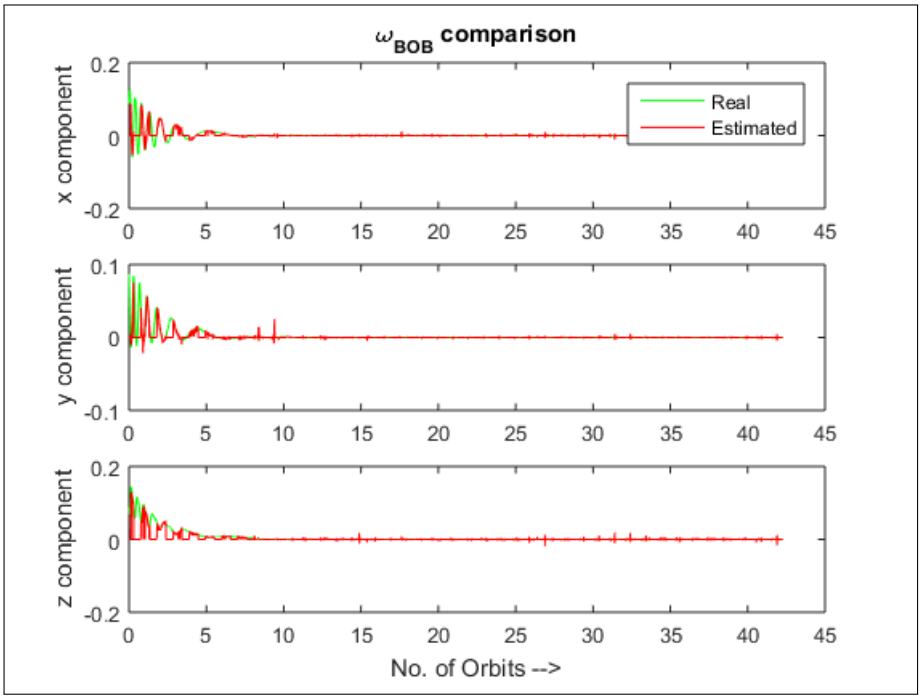

Figure 5.14: Rate of orbital frame w.r.t body frame expressed in body frame, estimated v/s real

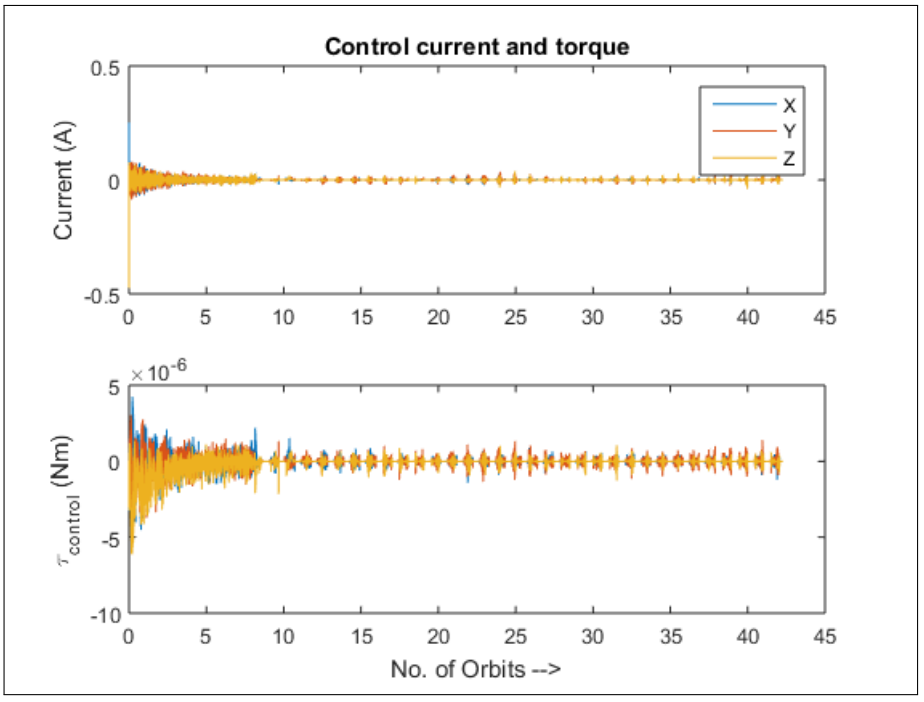

Figure 5.15: Control current and torque

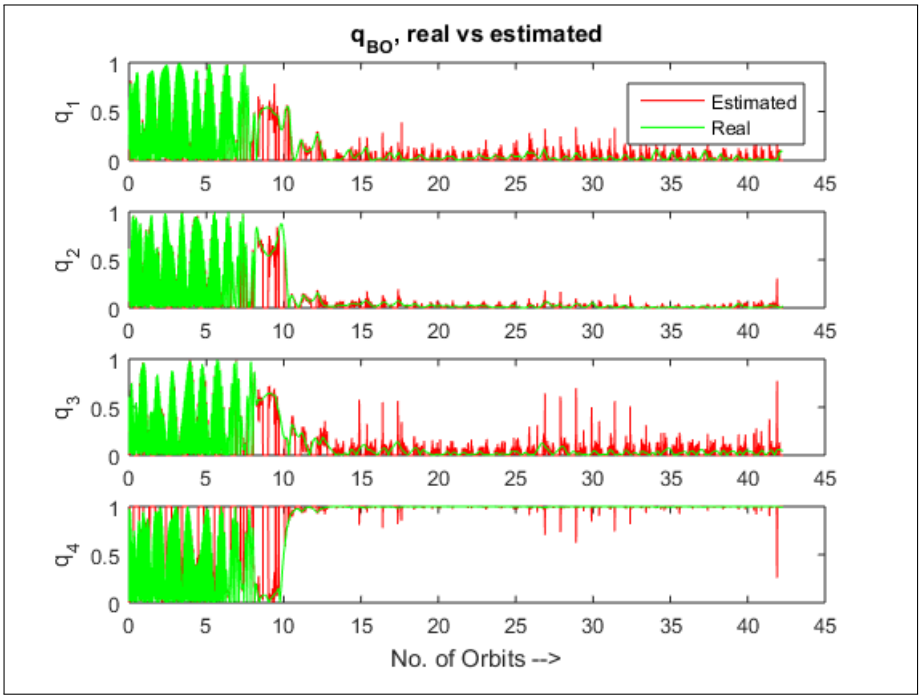

Figure 5.16: Quaternion of orbital frame w.r.t body frame

Case 2: The whole inertia matrix is scaled by a factor of 0.5.
Initial Angular rates: [5 5 5] deg/s along the X,Y and Z body axes respectively.
Initial Angular rates: [5,5,5] deg/s along the X,Y,Z body axes respectively
Initial Euler angles: 20^0 roll, 140^0 pitch, 80^0 yaw

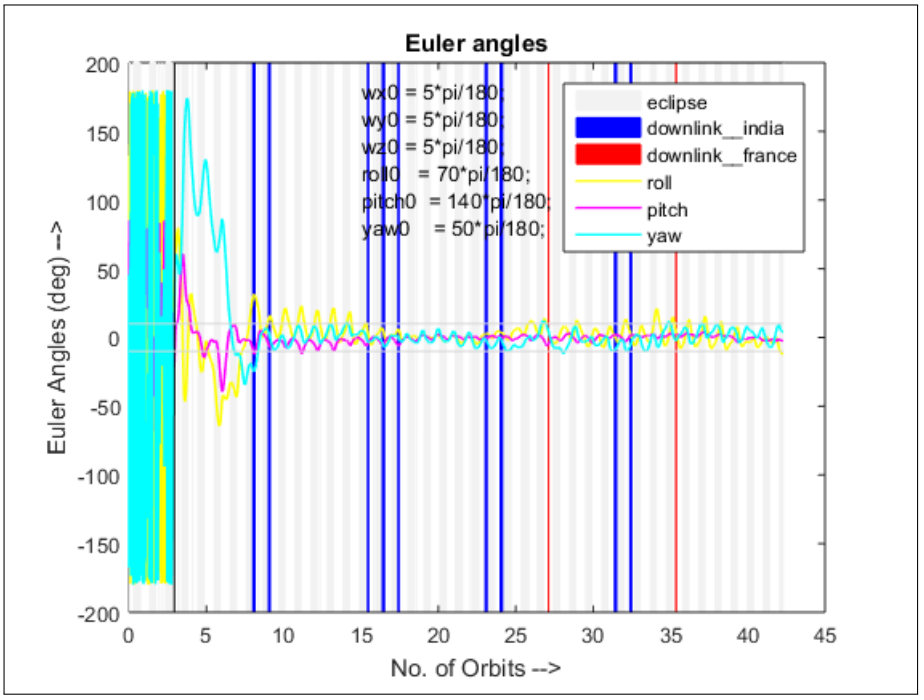

Figure 5.17: Euler angles

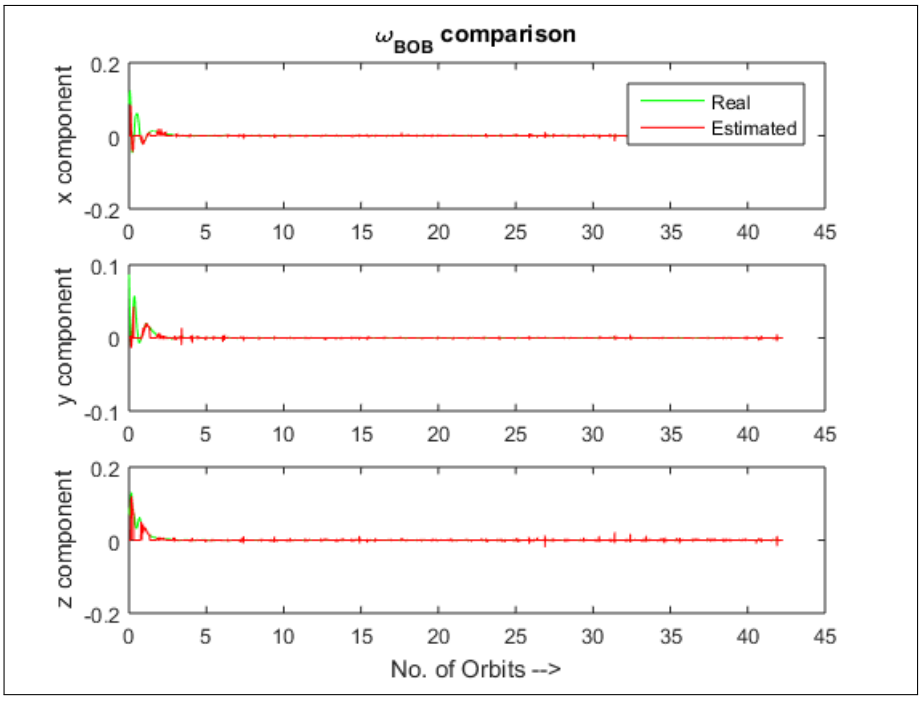

Figure 5.18: Rate of orbital frame w.r.t body frame expressed in body frame, estimated v/s real

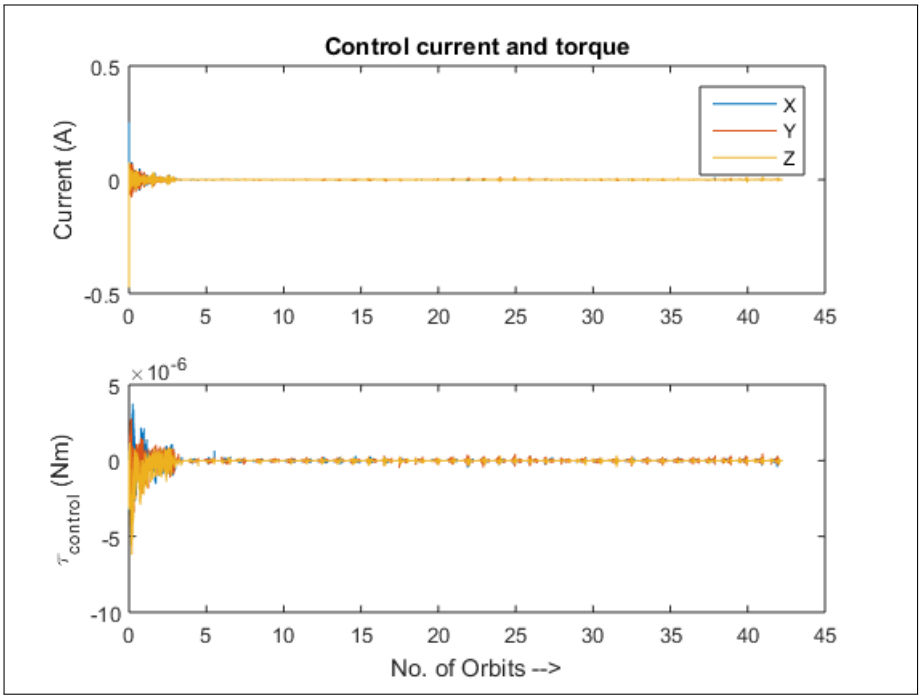

Figure 5.19: Control current and torque

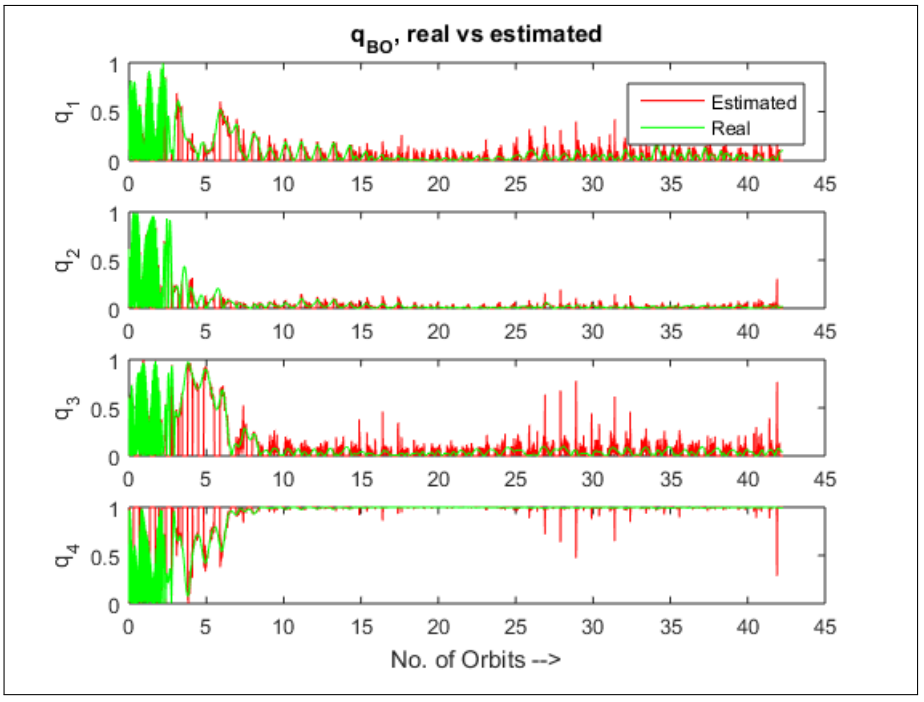

Figure 5.20: Quaternion of orbital frame w.r.t body frame

Case 3: The cross inertia terms are multiplied by 2 to take into account any deviation from the mass symmetry of the satellite. Beyond this factor, the controller cannot bring the rates within $\pm\ 10^0$.
Initial Angular rates: [5,5,5] deg/s along the X,Y,Z body axes respectively
Initial Euler angles: 20^0 roll, 140^0 pitch, 80^0 yaw

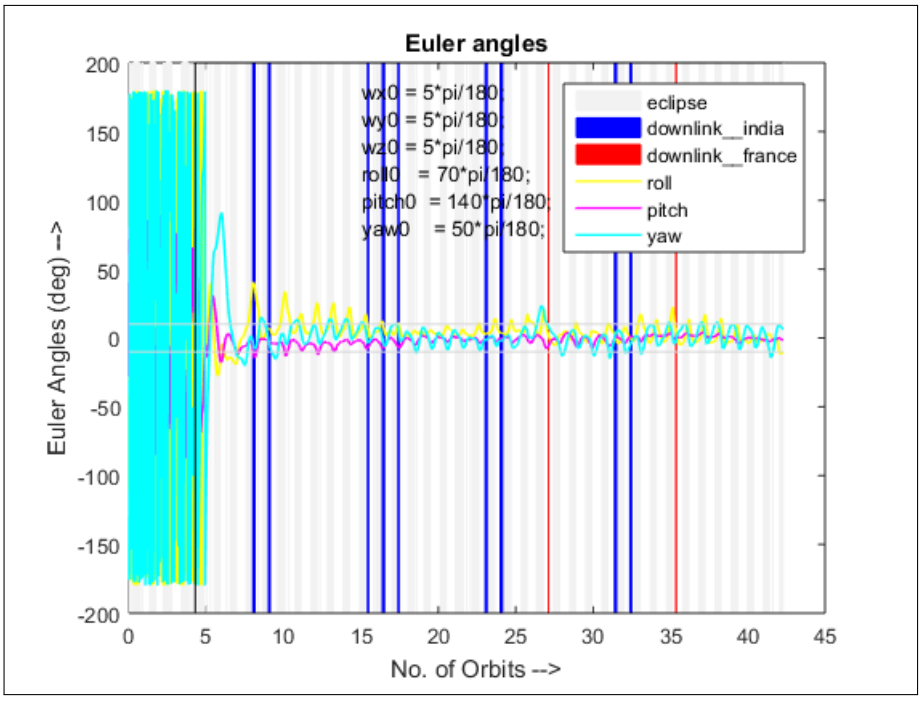

Figure 5.21: Euler angles

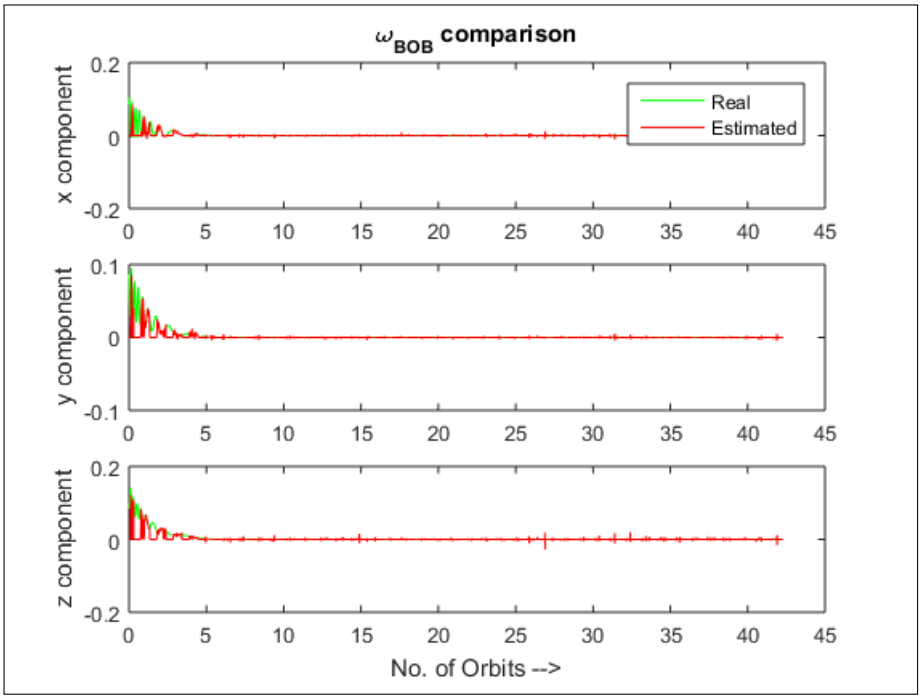

Figure 5.22: Rate of orbital frame w.r.t body frame expressed in body frame, estimated v/s real

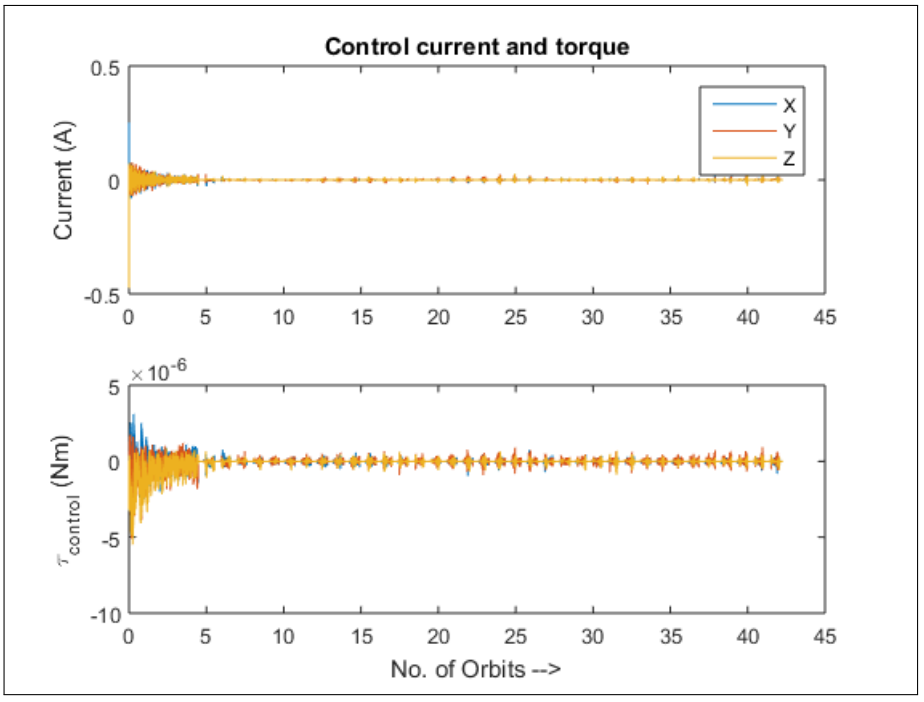

Figure 5.23: Control current and torque

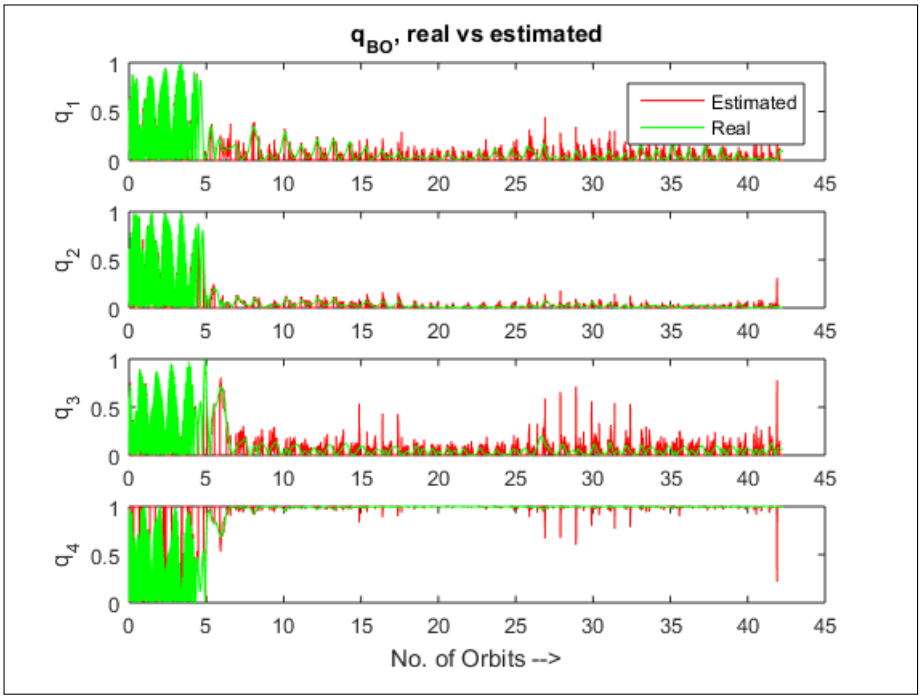

Figure 5.24: Quaternion of orbital frame w.r.t body frame

5.4 Monte Carlo Simulations

Monte Carlo simulations were carried out to verify that the nominal mode controller can stabilize the Euler angles within the required limits for any starting combination of Euler angles with rates within the limits required for end of detumbling.
The 1st test run was conducted with a set of 100 Euler angles which were generated using the random number generator. The control law simulation was run with only the nominal mode controller active for 20 orbits. The checking criterion was the maximum value of any Euler angle in the last 3 orbits.
The results were then plotted on a 3D domain representing the 3 Euler angles and the points were color coded as per maximum value of checking criterion.
The scatter plot of the cases run is shown below

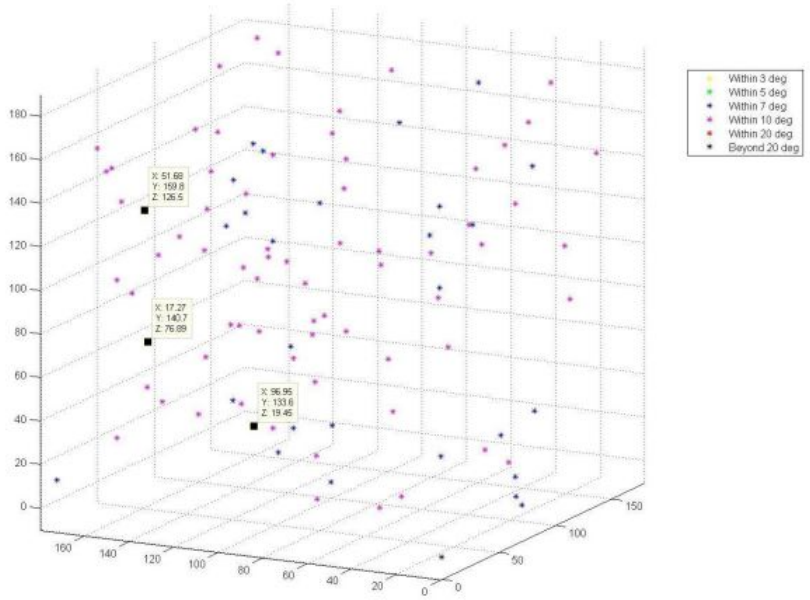

Figure 5.25: Euler angles from Monte Carlo simulations

The points marked on the plot indicate the points where one of the Euler angle was greater than 10. In the worst case the maximum value of the angle was 14 for the initial case corresponding to the Euler angle set [17.27 140.7 76.69] deg according to [Roll Pitch Yaw]. Further when the simulation was rerun, the angles were shown to be within 10 by the 20^{th}orbit.
A typical result for one of the cases in the simulation is shown below

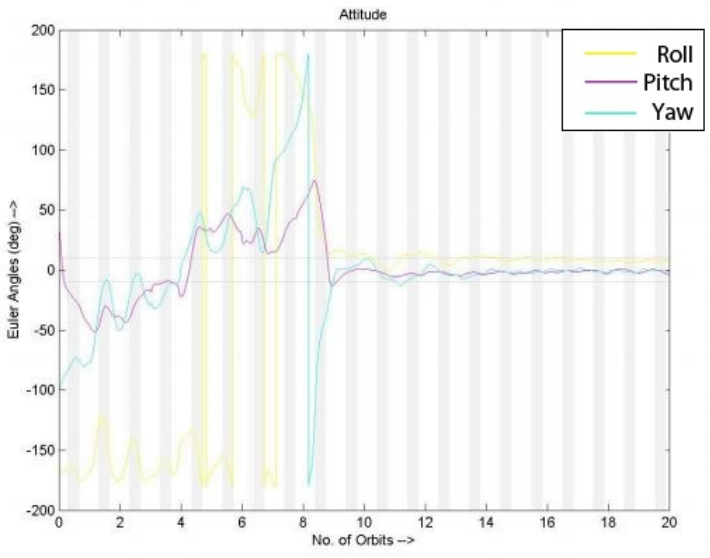

Figure 5.26: Euler angles from Monte Carlo simulations

The following are the results obtained from 500 cases

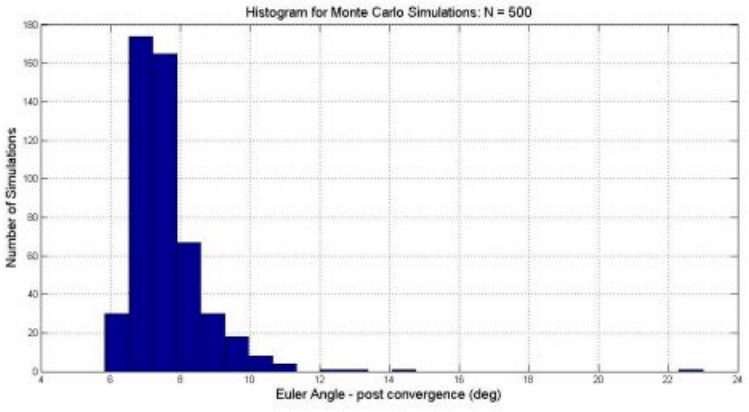

1

Figure 5.27: Histogram for Monte Carlo simulations, N = 500

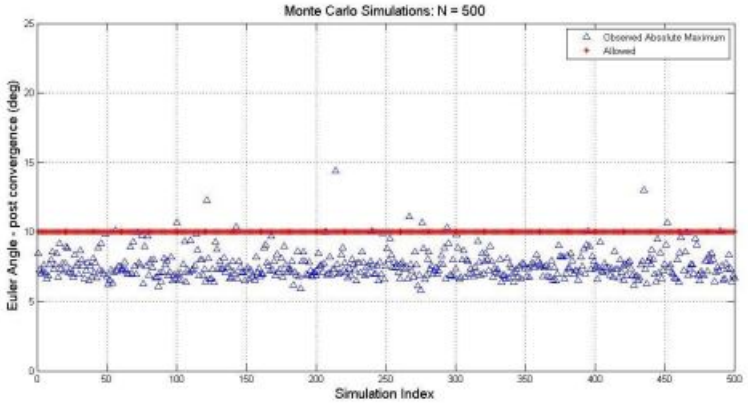

Figure 5.28: Post convergence Monte Carlo, N = 500

The following were the observations from the simulation

1. 15 cases of 500 were giving Euler angles post 20 orbits > 10 deg
2. Out of this 15 cases ONLY 5 were > 11 deg
3. Out of this 05 cases ONLY 1 was > 15 deg [Initial angles : -9.54 -136.73 -178.35]

The 2nd test run was conducted with a set of 100 initial Euler rates between 5 deg/s and 12 deg/s which were generated using the random number generator. The control law simulation was run with only the nominal mode controller active for 40 orbits. The checking criterion was the maximum value of any Euler angle in the last 3 orbits.
The scatter plot of the cases run is shown below.

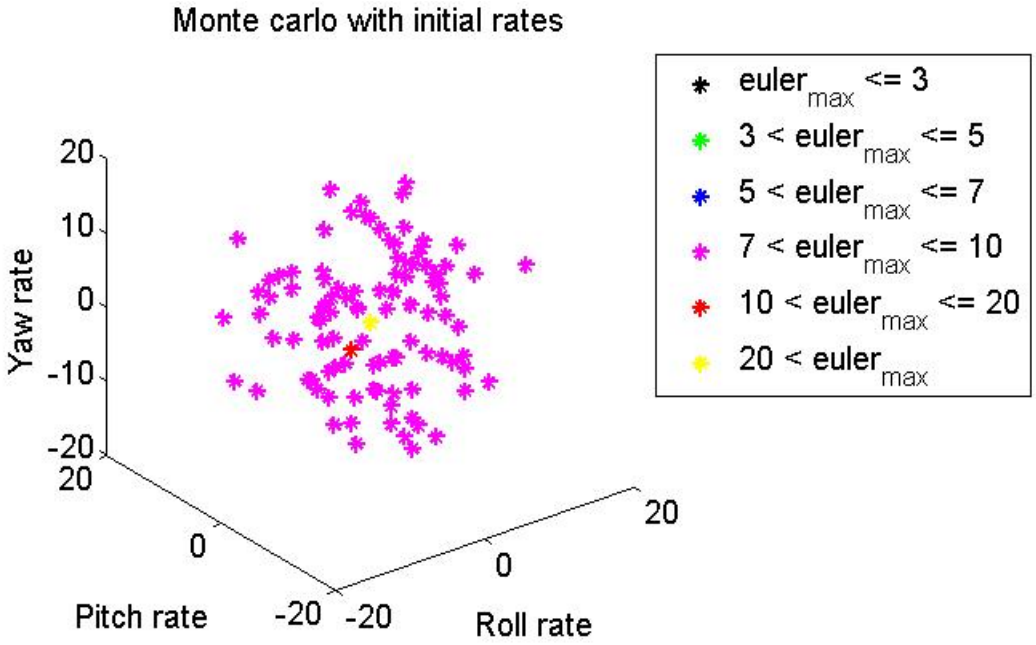

Figure 5.29: Monte Carlo with initial rates, 100 cases and 40 orbits

The following were the observations from the simulation

1. 98 cases out of 100 had Euler angles between 7 and 10 degrees
2. Only 1 case had Euler angles between 10 and 20 degrees (15.3 degrees) [Initial rates :[-7.58,-6.62,2.07]]
3. Only 1 case had Euler angles greater than 20 degrees [Initial rates :[0,0,0]]

Chapter 6

Battery Simulations

6.1 Introduction

The battery power simulink model essentially incorporates the modeling of power consumption from battery by the various loads and the power generation through solar panels with the attitude determination and controls model. The conditions for charging and discharging are determined by the voltage level of the battery and the differential power available or consumed.

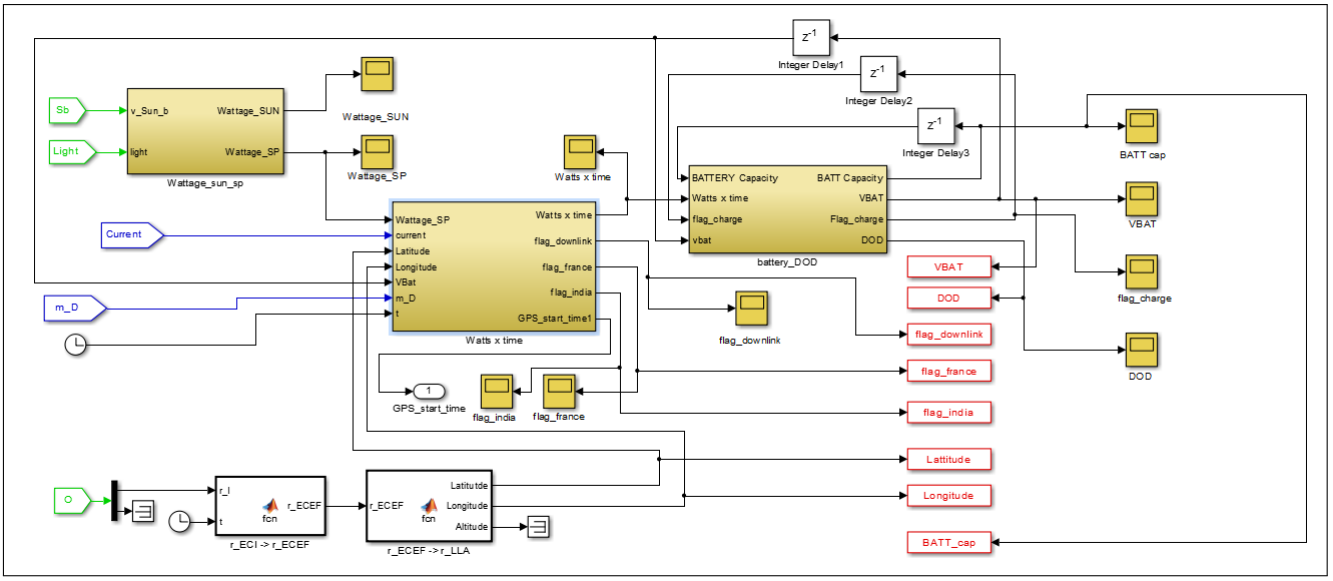

Figure 6.1: Battery simulation block

6.2 Power from solar panels

The simulink model for power generation through solar panels is as follows

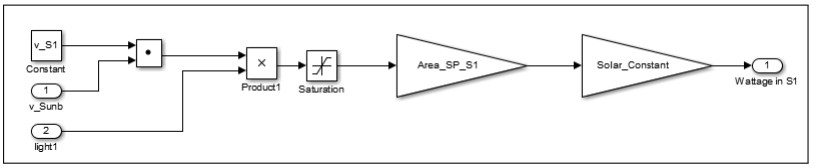

Figure 6.2: Simulation of power through solar panel

- The angle between the sun vector and the area vector of the solar panel face is determined by taking their dot product. The light flag determines whether the satellite is in light or eclipse phase.
- The solar intensity on the panel face can be determined using Lambert's cosine law $I = I_0 \cos(\theta)$
  where I_0 denotes the normal intensity
- The total solar power is the sum of the solar power available from all the faces multiplied by the efficiency of the solar panel (0.16).

6.3 Charging/Discharging of Battery

Table 6.1 shows the load values for calculation of power consumption. This does not include power requirement of magnetorquer as it is calculated in the MATLAB code which runs the attitude determination and controls simulations. The condition for battery charging

Power Supply	Supply Voltage (V)	Load Current (mA)	Load Power (W)
Beacon	5.00	548.60	2.74
Downlink	5.00	460.82	2.30
Torquer	3.60	865.70	3.12
OBC	3.30	24.77	0.08
GPS	5.00	400.10	2.00
Magnetometer	8.40	35.00	0.29
Miscellaneous	8.40	127.34	1.07
Total Power Consumption			**11.61**

Table 6.1: Power Consumption

depending on the cell voltage and the power from solar panels is as follows:

- Incoming solar power greater than power consumption AND
- Cell voltage less than 4.1 V if battery is in discharging mode in previous time step OR
- Cell voltage less than 4.2 V if battery is in charging mode in previous time step

6.4 GPS power consumption calculation

- Start the GPS when the average of moment is small enough (0.04 Nm/T) because on-board the starting of GPS is a requirement of mode switching.
- GPS must be off in eclipse region because of power constraints.

- In light region, GPS is switched on periodically after every 10 minutes and kept on for 1.5 minutes.
- The data of magnetic moment is very noisy, so filter (taking avg. of all the values) has to be used so that we can put a threshold (0.04 Nm/T) on that modified magnetic moment to start GPS.
- The switching from detumbling to nominal mode is decided by the estimated angular rates.

6.5 Downlink power consumption calculation

- Downlink takes place when the satellite is overhead India and Paris i.e. within a circle of radius 25 degrees centered at (22.58 lat,82.76 lon) degrees and a circle of radius 9 degrees centered at (48.8 lat,2.33 lon) degrees respectively.
- When power left in the battery is below a threshold (3.75), there is no downlink.
- Downlink does not take place in eclipse as angular rates are high and the position data has error in it since the GPS is switched off during eclipse

6.6 Simulation results

Detumbling mode is characterized by high angular rates and hence power generation through solar panels will take place with a lower efficiency in detumbling than in nominal mode. Accordingly, simulations are carried out for two cases with altitudes 500, 600, 700, 800 km with initial angular rates of [5,-5,5] deg./s:

1. The battery does not get charged at all in detumbling mode (worst case scenario)
2. The power generation of solar panels in detumbling mode takes place with an efficiency lower than that in nominal mode. The efficiency is taken as 50 % of the efficiency of nominal mode i.e. 8 %.

The initial DOD is determined by the current drawn by the electric switch SNAP circuit. Since electrical switch SNAP uses only 100 μA current, the battery will lose less than 0.036 % of its charge per day. Even in the case of delayed launch of one month or so, battery will drain approximately 1 % of its charge. Hence, corresponding to this worst case scenario, the initial DOD is taken to be 0.01. The following are the essential outputs obtained:

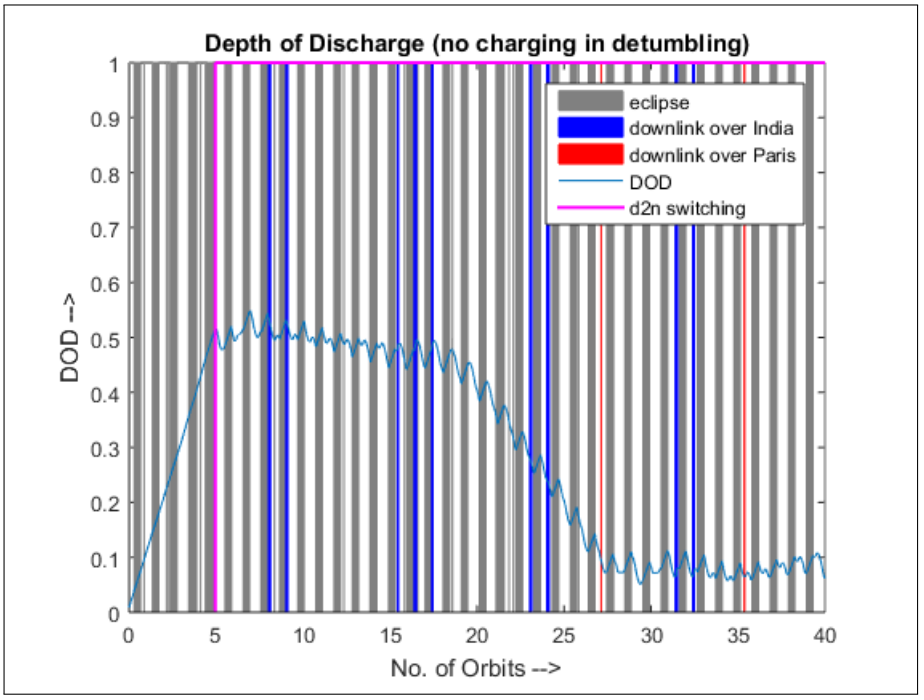

Figure 6.3: Depth of discharge for altitude 500 km (No charging in detumbling)

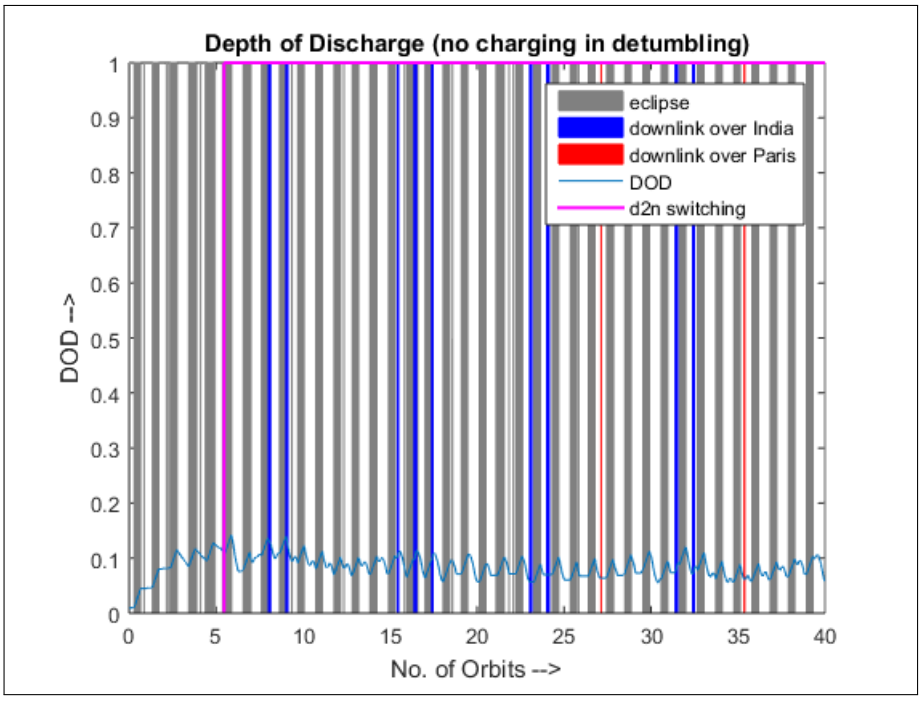

Figure 6.4: Depth of discharge for altitude 500 km (Charging with 8 % efficiency)

6.6.1 Inference

- DOD value reaches to a maximum of 0.15 in the case of charging during detumbling and 0.55 in the absence of charging during detumbling.
- In the case of no charging during detumbling, DOD reaches upto 0.55 after initial detumbling. But after about 20 orbits, it starts to decrease and then remains within 0.15 for subsequent orbits.
- In the case of charging during detumbling, the DOD does not shoot up to a high value during initial detumbling
- The actual scenario will be somewhere between the two cases, since the efficiency of charging during detumbling will steading increases as the angular rates continue to decreases. So, even for the worst case scenario, DOD is within 55 %.

Chapter 7

External torque simulations

7.1 Introduction

The environmental model which includes the aerodynamic torque, gravity gradient torque and torque due to solar radiation pressure is an approximate model of the external torques acting on the satellite. Given the dimensions of our satellite and the nature of its orbit (Low earth orbit), other external torques like luni-solar gravitational torque can be neglected. But in the environment of the space sudden changes like solar storms may cause the torques to increase in magnitude and also may result in time varying torques acting for short durations.
The purpose of these simulations was to model the complete failure of the satellite due to the action of unmodelled external torques. The various scenarios of external torques considered might not act in the actual space environment but it was intended to find out the probable scenarios in which the satellite will enter a continuous detumbling mode.

7.2 Case 1 - Scaling up of the modeled torques

Since the models are approximate and are dependent on approximate constants, there's a possibility of scaling up of the torques in the actual scenario even though the scaling would be low.

1. Scaling factor = 3
   Note - The order of modeled torque is 10^{-9}

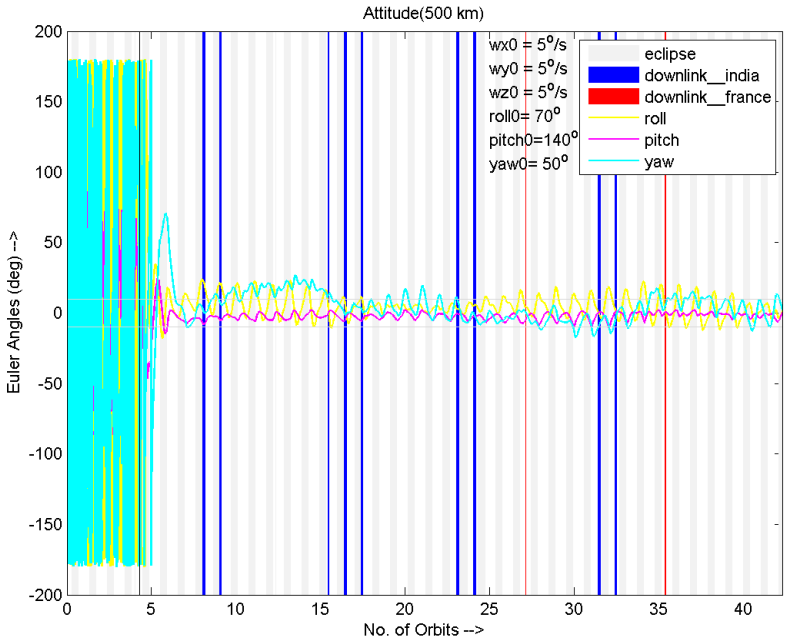

Figure 7.1: Euler angles for case 1 simulation; scaling factor = 3

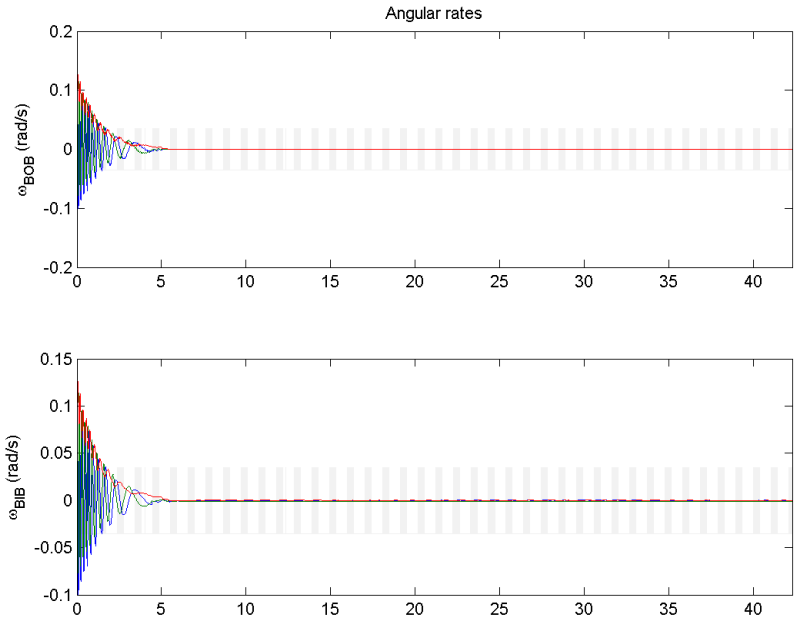

Figure 7.2: Angular rates for case 1 simulation; scaling factor = 3

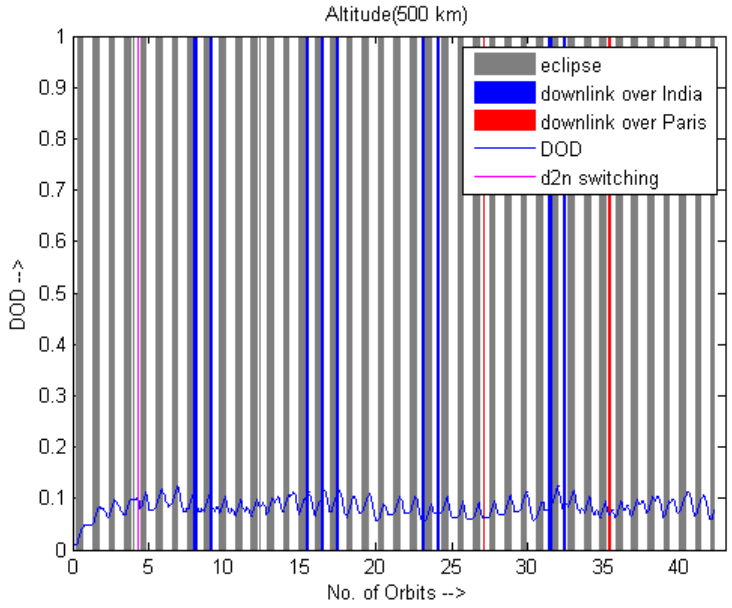

Figure 7.3: Depth of discharge for case 1 simulation; scaling factor = 3

2. Scaling factor = 10

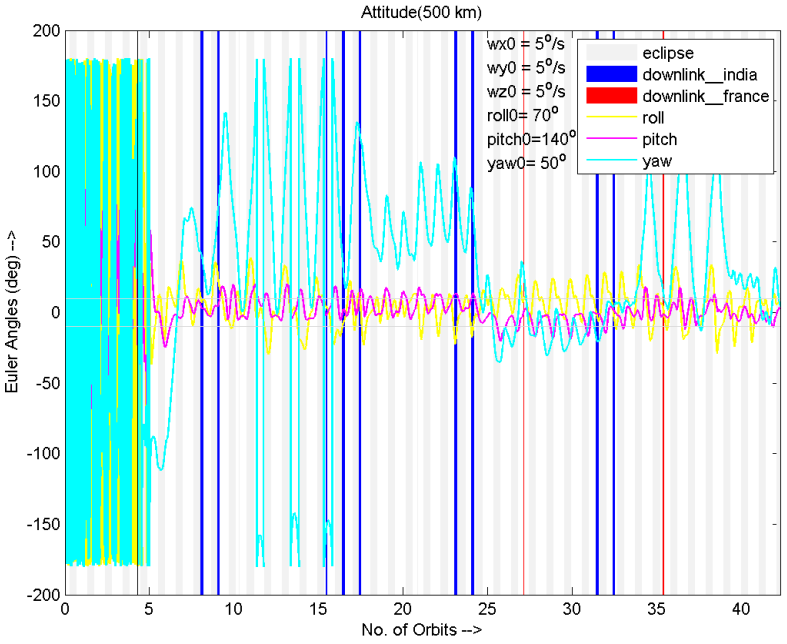

Figure 7.4: Euler angles for case 1 simulation; scaling factor = 10

7.2.1 Conclusions

- The Euler angles go beyond 10 degrees when the scaling factor is 3 or more, reaching up to about 100 degrees.
- But even though, the angles increase by a large amount, the rates are still stabilized and hence the DOD is low since switching does not take place. This is because the magnitude of the torque is constant with time from the beginning and hence does not affect the rates.

7.3 Case 2 - Linearly varying torque

A linearly varying torque with a positive randomly varying slope is added when the satellite is in eclipse mode and allowed to decay linearly when it enters light mode. This is because the control law is switched off during the eclipse mode (if the rates are stabilized) and hence the rates may increase significantly if a torque of varying magnitude acts during that time.

1. Slope = $10^{-9}\times$ random number between 1 and 9

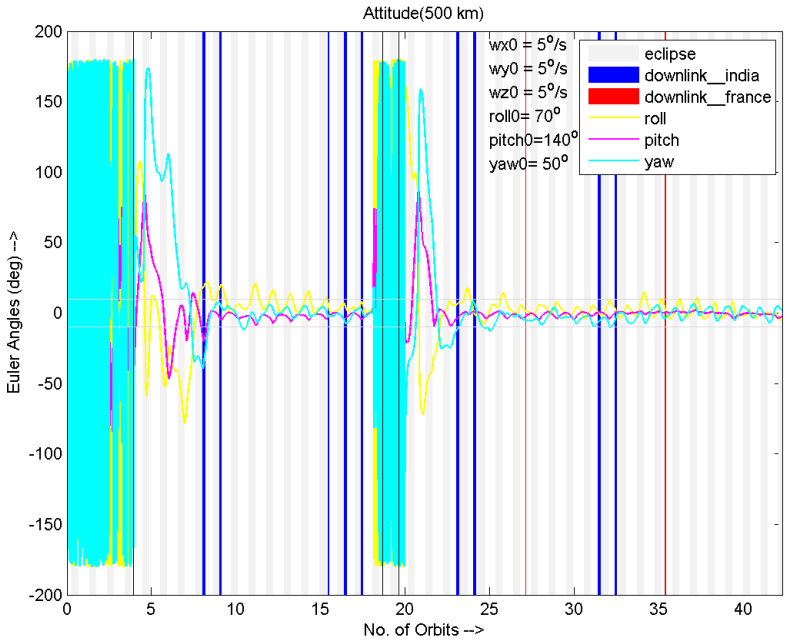

Figure 7.5: Euler angles for case 2 simulation; Slope = 10^{-9}

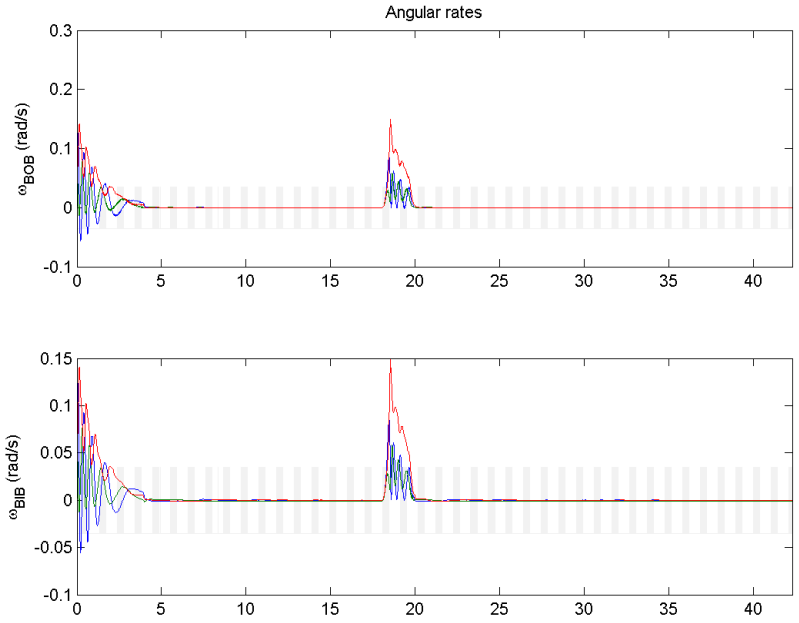

Figure 7.6: Angular rates for case 2 simulation; Slope = 10^{-9}

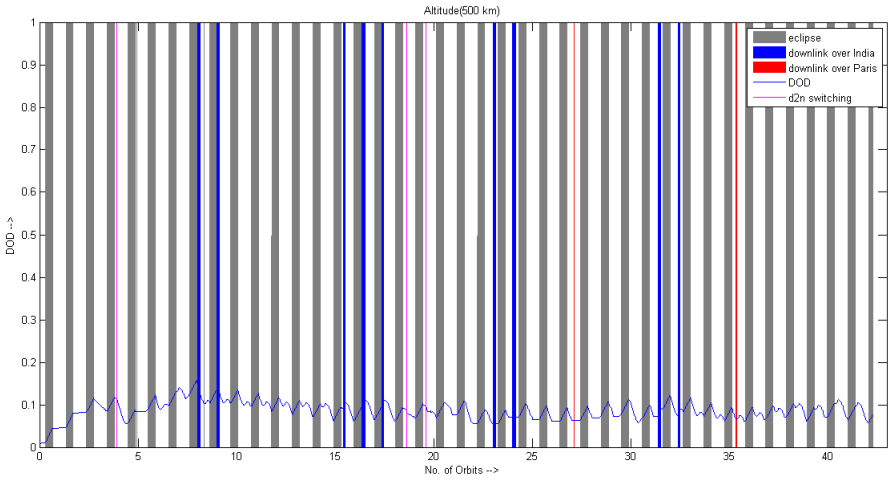

Figure 7.7: Depth of discharge for case 2 simulation; Slope = 10^{-9}

2. Slope = $10^{-7}\times$ random number between 1 and 9

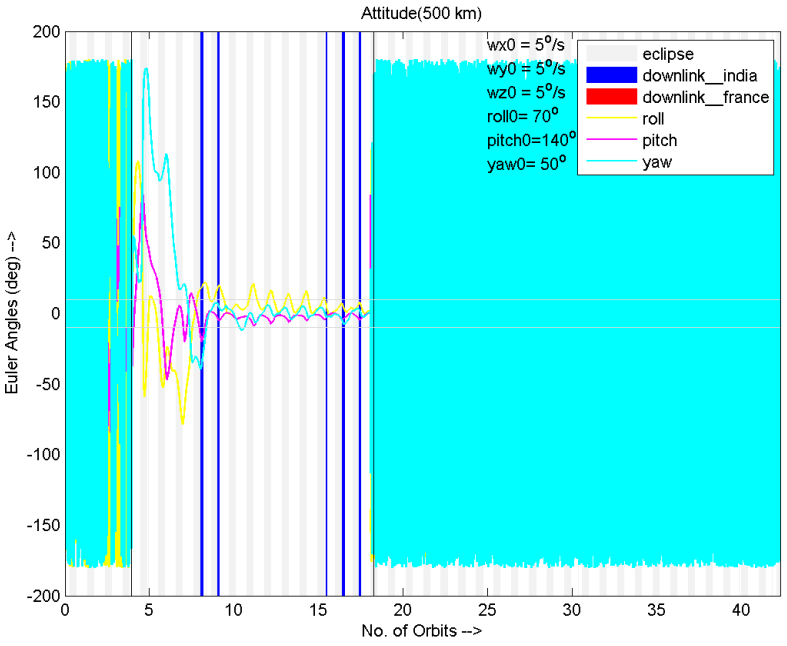

Figure 7.8: Euler angles for case 2 simulation; Slope = 10^{-7}

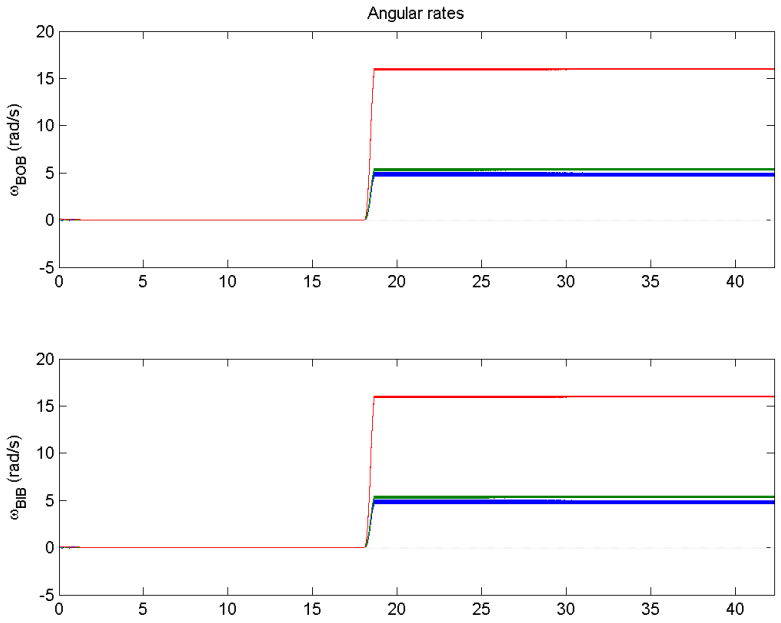

Figure 7.9: Angular rates for case 2 simulation; Slope = 10^{-7}

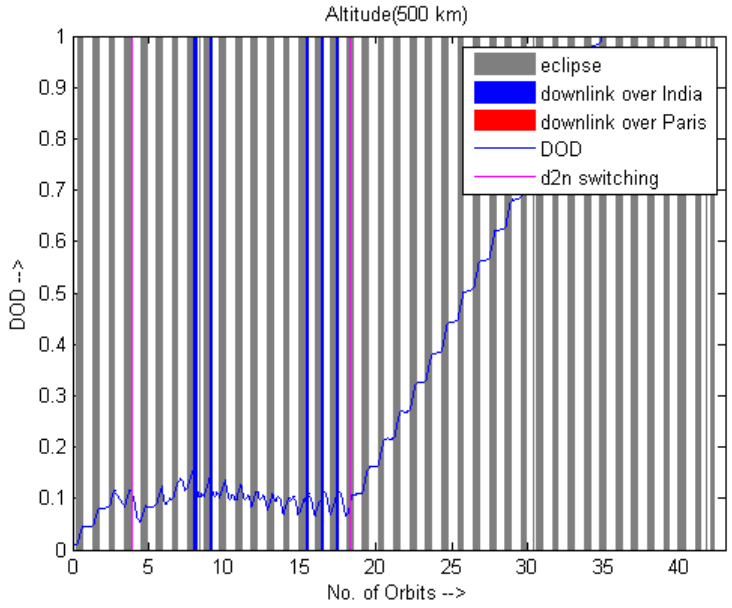

Figure 7.10: Depth of discharge for case 2 simulation; Slope = 10^{-7}

7.3.1 Conclusions

- We see that for a slope of 10^{-7}, the satellite is in continuous detumbling and the DOD reaches 1 and hence this scenario models the complete failure of the satellite.